Applied Radiation and Isotopes 153 (2019) 108797

Contents lists available at ScienceDirect

Applied Radiation and Isotopes

journal homepage: www.elsevier.com/locate/apradiso

Review

Stimulated luminescence emission: From phenomenological models to master analytical equations

George Kitis[a,*], George S. Polymeris[b], Vasilis Pagonis[c]

[a] Aristotle University of Thessaloniki, Physics Department, Nuclear Physics and Elementary Particles Physics Section, 54124, Thessaloniki, Greece
[b] Institute of Nuclear Sciences, Ankara University, 06100, Beşevler, Ankara, Turkey
[c] McDaniel College, Physics Department, Westminster, MD, 21157, USA

HIGHLIGHTS

- The analytical solutions of elementary stimulated luminescence models is reviewed.
- The analytical solutions are given in the form of master equations.
- A single master equation represents all stimulated luminescence phenomena at any stimulation mode.
- The transformation of analytical equations to into forms suitable for curve fitting analysis is reviewed. .
- Applications of analytical equations to experimental results are reviewed.

ARTICLE INFO

G.K. dedicates this article to his mentor Prof. Adreas Paterakis.

Keywords:
Thermoluminescence
Optically stimulated luminescence
Infra
Red stimulated luminescence
Radiation dosimetry
Dating
Glow curve analysis

ABSTRACT

This paper reviews developments in phenomenological models of stimulated luminescence phenomena. A set of five master equations is presented, which describe a wide variety of stimulated luminescence signals: thermoluminescence, isothermal luminescence, optically stimulated luminescence and infrared stimulated luminescence. Both delocalized and localized models are reviewed, and analytical solutions are presented for these models. The master equations are tested against the solutions of the differential equations in the models, as well by fitting experimental data for a variety of luminescencent dosimetric materials. Three out of the five master equations involve the Lambert W(z) function, thus establishing this function as the theoretical cornerstone of the phenomenological luminescence models. The applicability of the superposition principle is discussed, in connection with computerized curve deconvolution analysis.

1. Introduction

The interaction of ionizing radiation with both natural and artificial inorganic materials makes these materials suitable to act as radiation detectors. An important family of radiation detectors, called passive detectors, is based on the existence of localized energy levels within the forbidden energy band. These energy levels are created by the presence of imperfections and impurities in the crystal lattice, or by the irradiation of these materials in nature or in the laboratory.

In the framework of the phenomenological energy band model of solids, the irradiation process ionizes the atoms, creating electrons in the conduction band and holes in the valence band. The electrons from the conduction band are trapped in electron traps and the holes in hole traps (which can also act as luminescence centers) within the forbidden band.

After irradiation the system is in an excited state, and the lifetime of these excited states in nature varies widely from microseconds to billions of years. When the material is thermally or optically stimulated in the laboratory, the trapped electrons are released and may eventually recombine with holes at luminescence centers, thus causing the emission of light from the sample. The principal properties making the material a dosimeter are: (a) During irradiation a functional relationship must exists between the number of electrons trapped in the material and the irradiation dose. (b) During the heating stage a function relationship must exist between the photons emitted and the trapped electrons in (a). Finally, due to (a) and (b) a functional relation must exist between the emitted photons and irradiation dose.

Various stimulation methods are commonly used in the laboratory

* Corresponding author.
E-mail address: gkitis@auth.gr (G. Kitis).

https://doi.org/10.1016/j.apradiso.2019.05.041
Received 3 April 2019; Received in revised form 15 May 2019; Accepted 20 May 2019
Available online 05 July 2019
0969-8043/

to liberate the trapped electrons, and these methods generate different stimulated luminescence (SL) signals. When the stimulation is thermal, the phenomenon is called Thermoluminescence (TL) or thermally stimulated luminescence (TSL). When the stimulation is optical using visible light, one is dealing with optically stimulated luminescence (OSL). Finally when the stimulation takes place with infrared photons, this is called infrared stimulated luminescence (IRSL). Subcategories of these effects are also commonly used, depending upon the stimulation rate. In the case of TL signals, common experimental heating functions are linear, hyperbolic and exponential heating functions. In the case of OSL and IRSL, the stimulation rate can be linear leading to Linearly modulated OSL and IRSL (LM-OSL and LM-IRSL). Alternatively, stimulation can take place with a constant light intensity, leading to continuous wave OSL and IRSL signals (CW-OSL and CW-IRSL). Additionally, the optical stimulation can be in a pulsed mode, giving rise to pulsed OSL and pulsed IRSL signals (POSL and PIRSL). For a review of these phenomena the readers are directed to several available excellent textbooks and review articles on luminescence dosimetry and its applications (Braunlich, 1979; Chen and Kirsh, 1981; Horowitz, 1984; Böhm and Scharmann, 1981; Chen and McKeever, 1997; Martini and Meinardi, 1997; McKeever and Chen, 1997; Furetta and Weng, 1998; Bøtter-Jensen et al., 2003; Furetta, 2003; Pagonis et al., 2006; Chen and Pagonis, 2011; Yukihara and McKeever, 2011).

Examples of SL curves obtained with various stimulation modes are shown in Fig. 1. During a TL experiment one records the light intensity as a function of temperature, and the total signal is termed a TL glow curve (Fig.1ab). During a LM-OSL experiment, the light intensity is recorded as a function of time, while increasing the stimulation linearly with time, thus obtaining a peak-shaped LM-OSL curve (Fig. 1c). During CW-OSL or CW-IRSL experiments the light intensity is constant, resulting in a CW-OSL decay curve (Fig. 1d).

The complexity of all these curves is obvious in Fig. 1, so the fundamental question is how to extract the physical information from these experimental curves.

In general, researchers would like to extract the following specific information:

- The basic physical parameters of the energy level responsible for the emission of light.
- The intensity of the light emitted during each SL effect.

All SL phenomena can be described by phenomenological models, which are described by systems of differential equations.

The main goal of this article is to provide a review and synthesis of several phenomenological models commonly used to describe luminescence signals, similar to those shown in Fig. 1. Both delocalized and localized models are reviewed, and analytical solutions are presented for five general models in the form of analytical equations termed *master equations*. The term “master equations” is used here to describe *analytical* equations which can be used to describe a whole group of possible procedures in stimulated luminescence experiments. However, the meaning of the term “master equations” in this review paper is different from the same term used in chemistry and other fields of science, which are a set of *differential* equations describing time-dependent transitions between different states of the system.

The five master equations in this paper were tested against the solutions of the differential equations in the models, as well by fitting experimental data for a variety of luminescencent dosimetric materials.

The next section discusses the overall organization of this paper.

2. How this review paper is organized

The paper is organized as follows. Section 1 provides an overview of the types of luminescence signals which are commonly used for luminescence dosimetry and luminescence dating and other applications (Daniels et al., 1953; Bos, 2017).

In Section 3 we present the simplest delocalized phenomenological model in luminescence, which is based on one trap and one recombination center (OTOR). Two limiting cases are derived within this model by using the quasi-equilibrium conditions, namely first order and second order kinetics. The analytical solution of the OTOR model is derived next, based on the Lambert function; this analytical solution constitutes the *first master equation*, which describes a variety of stimulated luminescence signals.

Section 4 presents the more general interactive multi-trap system model (IMTS), and its more restricted version known as the non-interacting multi-trap system (NMTS). Under special physical assumptions, the NMTS model is shown to lead to the mixed-order kinetics

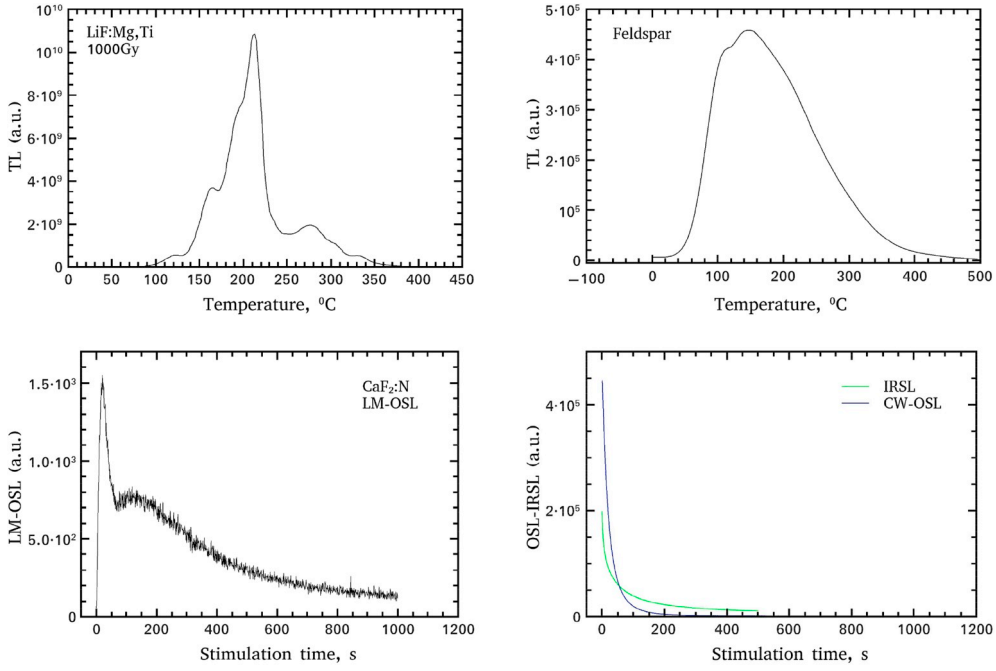

Fig. 1. Typical experimental curves from stimulated luminescence phenomena: (a) and (b) TL glow curves, (c) LM-OSL signals and (d) CW-IRSL and CW-OSL signals.

model (MOK), which is a linear combination of the equations for first and second order kinetics. The analytical solution of the MOK model constitutes the *second master equation*. The analytical solution to the NMTS model is also obtained in terms of the Lambert function, and is the *third master equation*.

Section 5 contains the simple localized transition model (SLT). This model is based on transitions occurring between three energy levels, namely the ground and excited state of a localized electron trap, and the recombination center. When the recombination probability is constant, the analytical solution of the SLT model is obtained in terms of the Lambert function, and this constitutes the *fourth master equation*.

The general presentation of the master equations is completed in Section 6, where we consider a tunneling localized transition model (TLT). This model is based on a variable recombination probability, resulting from a distribution of distances between the traps and recombination centers in the crystal. The analytical solution of the TLT for freshly irradiated samples is the *fifth master equation* in this paper.

Sections 7-9 present transformation equations for the analytical master solutions presented in Sections 3-6. Specifically the analytical equations are transformed into new equations containing two parameters which can be determined directly from the experimental data, namely the maximum luminescence intensity (I_{max}) and the corresponding time or temperature where the maximum occurs (t_{max} or T_{max}). The transformation equations are presented for the five master equations, and for a variety of luminescence signals.

Section 10 contains the mathematical formalism of the well known empirical general order kinetics (GOK) model. Analytical solutions of the GOK model are presented for several luminescence phenomena. This section includes a discussion of the relationship between the first master equation for the OTOR model, and the empirical GOK equations. The discussion shows that the gap between first and second order kinetics phenomena can be bridged using *either* the Lambert OTOR analytical solutions, *or* the empirical general order kinetics. The section also emphasizes the direct relationship between the retrapping rate (R) in the OTOR model, and the empirical kinetic order constant b (see section 10.8).

Section 11 also presents two specialized mathematical techniques, which have been used to transform a featureless luminescence signal into a peak-shaped curve. Section 12 contains a general discussion of the Superposition principle (SP) as it applies to luminescence models, and a consideration of the influence of competition effects in the applicability of the SP.

Finally, the paper concludes in Section 13 with a summary of the five master equations and their application in analyzing experimental luminescence signals.

3. The OTOR model: first master equation

The most common and simplest phenomenological energy band model is the OTOR model, shown as a schematic energy diagram in Fig. 2. The diagram shows one trapping state and one kind of recombination center, and the arrows indicate the delocalized transitions in the model.

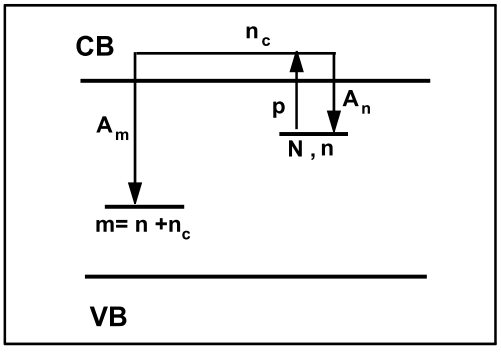

Fig. 2. Energy band diagram for the OTOR model.

A complete presentation of the OTOR model must include three stages which correspond to events taking place in a typical luminescence experiment. These stages are irradiation, relaxation and read-out stages.

We now describe the differential equations for each of these three stages.

3.1. The irradiation stage

The differential equations governing the traffic of electrons between the trapping level, the recombination center and the conduction band in the OTOR model are (Adirovitch, 1956; Halperin and Braner, 1960; Chen and Kirsh, 1981; Chen and McKeever, 1997):

$$\frac{dn}{dt} = A_n(N-n)n_c, \tag{1}$$

$$\frac{dm}{dt} = B(M-m)n_v - A_m m n_c, \tag{2}$$

$$\frac{dn_c}{dt} = X - A_n(N-n)n_c - A_m m n_c, \tag{3}$$

$$\frac{dn_v}{dt} = \frac{dn}{dt} + \frac{dn_c}{dt} - \frac{dm}{dt}. \tag{4}$$

Here and $m\,(cm^{-3})$ are the concentrations of electrons in traps and of holes in recombination centers respectively, and N and $M\,(cm^{-3})$ are the total concentrations of trapping states and recombination centers .$n_c(cm^{-3})$ and $n_v(cm^{-3})$ are respectively the concentrations of free electrons and holes. $A_n(cm^3s^{-1})$ is the retrapping coefficient of electrons, $A_m(cm^3s^{-1})$ the recombination coefficient of electrons, and $B(cm^3s^{-1})$ the trapping coefficient of holes in centers. $X(cm^{-3}s^{-1})$ is proportional to the dose-rate of excitation, and actually denotes the rate of production of electron-hole pairs by the excitation irradiation process (per unit volume and per second). A detailed listing of the parameters in the IMTS model is given in Table 1.

This set of equations cannot be solved analytically. From this point on, one can proceed by making simplifying assumptions to get some general approximate behavior of the dependence of the concentrations of trapped carriers on the dose. More often, one has to solve numerically the set of equations for a chosen set of parameters.

It is to be noted here that in the TL/OSL literature one often finds the terms “trapping probability” or “recombination probability” for A_n, B and A_m (with units of cm^3s^{-1}). Although rather common, these terms

Table 1
Symbols, Units and physical meaning of the parameters used in phenomenological models based on *delocalized transitions*.

a/a	Symbol	Units	Physical meaning
1	e^-		Electrons freed by irradiation
2	h^+		holes freed by irradiation
3	n_c	cm^{-3}	Electron concentration in the conduction band
4	n_v	cm^{-3}	Electron concentration in the valence band
5	N	cm^{-3}	Concentration of available electron traps
6	n	cm^{-3}	Concentration of electrons trapped in N
7	M	cm^{-3}	Concentration of available hole traps
8	m	cm^{-3}	Concentration of holes trapped in M
9	N_d	cm^{-3}	Concentration of available TDDT
10	n_d	cm^{-3}	Concentration of electrons trapped in N_d
11	A_m	$cm^3\,s^{-1}$	Recombination coefficient
12	A_n	$cm^3\,s^{-1}$	Trapping coefficient in active trap
13	A_d	$cm^3\,s^{-1}$	Trapping coefficient in TDDT
14	A_h	$cm^3\,s^{-1}$	Trapping coefficient of holes in M
15	T	K	Absolute Temperature

are not very accurate. In fact, what is meant is that products like $A_m m$ or $A_n(N-n)$, having units of s^{-1}, and they represent transition rates per second. Another way to look at these coefficients is, for example, by stating that $A_m = \sigma_m v$ where σ_m is the cross section for recombination (in cm^2) and $v(cm/s)$ is the thermal velocity of the relevant free carrier.

3.2. The relaxation stage

At the end of excitation, we end up with finite concentrations of the free electrons (n_c) in the conduction band, and free holes (n_v) in the valence band. If we wish to mimic the experimental procedure of TL or OSL, we have to consider a relaxation time between the end of excitation and the beginning of heating or exposure to stimulating light. This is done by setting X to zero and solving Eqs. (1)–(4) for a further period of time, so that at the end of this time period both n_c and n_v are negligibly small. The final values of n, m, n_c, and n_v at the end of excitation are used as initial values for the relaxation stage. Similarly, we take the final values of these four functions at the end of relaxation period as initial values for the heating stage. One utilizes a certain heating function, e.g. linear heating in the form $T = T_o + \beta t$, where β is the constant heating rate. The same set of equations is being solved numerically with $X = 0$ and with the term on the right-hand side of Eq. (1) being more and more important as the temperature rises. On the other hand, it is usually assumed that during heating, $n_v \approx 0$.

3.3. The thermal or optical stimulation stage

The equations governing the process during thermal or optical stimulation are:

$$\frac{dn}{dt} = A_n(N-n)n_c - n\,p(t)\,, \tag{5}$$

$$\frac{dn_c}{dt} = n\,p(t) - A_n(N-n)n_c - A_m m n_c, \tag{6}$$

$$I(t) = -\frac{dm}{dt} = A_m m n_c, \tag{7}$$

$$\frac{dm}{dt} = \frac{dn}{dt} + \frac{dn_c}{dt}. \tag{8}$$

The charge neutrality condition is:

$$m = n + n_c. \tag{9}$$

The emitted light is associated with the recombination of free electrons with holes in recombination centers, and is given by Eq. (7).

The differential equations contain the term $p(t)$, which is a function representing the experimental stimulation mode. When the sample is thermally stimulated, the stimulated luminescence signal is called *Thermoluminescence* (TL) or thermally stimulated luminescence (TSL), and the function $p(t)$ is given by:

$$p(t) = s\,e^{-\frac{E}{kT(t)}}, \tag{10}$$

where E is the thermal activation energy of the trap, and $s\,(s^{-1})$ is the associated frequency factor. When the thermal stimulation takes place at a constant temperature T_D, the stimulated luminescence signal is called *prompt isothermal decay* (PID), and the function $p(t)$ is given by:

$$p(t) = s\,e^{-\frac{E}{kT_D}}. \tag{11}$$

When the stimulation is optical in nature and occurs with a source of constant light intensity, the stimulated luminescence is termed *continuous wave optically stimulated luminescence* (CW-OSL), and the function $p(t)$ is given by:

$$p(t) = \sigma\,I, \tag{12}$$

where $\sigma\,(cm^2)$ represents the optical cross section for the CW-OSL process, and $I\,(photons\ cm^{-2}\ s^{-1})$ represents the photon flux density.

When the optical stimulation takes place using a source with a linearly varying intensity, the stimulated luminescence is called *linearly modulated optically stimulated luminescence* (LM-OSL) and the function $p(t)$ is given by:

$$p(t) = \frac{\sigma\,I}{P}\,t, \tag{13}$$

where σ, I have the same meaning as in Eq. (12), and $P(s)$ is the total illumination time.

When the stimulation is in the form of infrared photons from a source of constant light intensity, the stimulated luminescence is called *continuous wave infrared stimulated luminescence* (CW-IRSL), and the function $p(t)$ is given by:

$$p(t) = \lambda = \sigma\,I, \tag{14}$$

where $\sigma\,(cm^2)$ represents the optical cross section for the CW-IRSL process, and $I\,(photons\ cm^{-2}\ s^{-1})$ represents the infrared photon flux density.

An important point to be made is, that solving the set of equations for the read-out stage (for either TL or OSL), without the initial solution of the equations during the excitation and just making a guess concerning the initial concentrations (prior to heating or optical stimulation) may not yield reliable results. Although in the present simple case of one trapping state and one kind of recombination center, one can expect at the end of relaxation that $n_o = m_o$, in more complicated situations where more levels are involved and which will be discussed later, making an arbitrary assumption about n_o and m_o as well as concentrations of the other relevant trapping states at the end of relaxation may not be compatible with the parameters of "these" states. For a discussion of this crucial topic see Lawless et al. (2005) and Sadek and Kitis (2017).

The development of analytical expressions explicitly defining the relationship between the stimulated luminescence intensity and temperature or time, requires some simplifying assumptions, with the most important being the quasi-equilibrium (QE) assumption, expressed as

$$\left|\frac{dn_c}{dt}\right| << \left|\frac{dn}{dt}\right|,\ \left|\frac{dm}{dt}\right|. \tag{15}$$

The QE assumption requires that the free electron concentration in the conduction band is quasi-stationary (Chen and McKeever, 1997). In practice, this means that the concentration of n_c is always much less than the concentration of n, or that $n \simeq m$. This allow us to set:

$$\frac{dn_c}{dt} = 0, \tag{16}$$

and the luminescence intensity is given by:

$$I(t) = -\frac{dm}{dt} \simeq -\frac{dn}{dt}. \tag{17}$$

Based on Eq. (16) and Eq. (6), the n_c value under the QE conditions is:

$$n_c = \frac{n\,p(t)}{A_n(N-n) + m\,A_m}. \tag{18}$$

By replacing n_c from Eq. (18) into Eq. (7) and since $n = m$, the following is obtained:

$$I(t) = -\frac{dm}{dt} = p(t)\,\frac{n^2\,A_m}{(N-n)A_n + n\,A_m}. \tag{19}$$

Eq. (19) is termed the general one trap (GOT) equation. When the GOT equation was first introduced by Adirovitch (1956) and by Halperin and Braner (1960), it was not possible to solve it analytically. The analytical solution was obtained close to 50 years later by Kitis and Vlachos (2013), and will be presented in section 3.4.

The OTOR model leads to first order kinetics, as a degenerate state for very weak retrapping ($A_n/A_m << 10^{-2}$), or for very strong

retrapping. For example, by assuming that $(N-n)A_n << nA_m$, Eq. (19) leads to the following differential equation, which expresses first order kinetics:

$$I = -\frac{dn}{dt} = n\,p(t).$$

For example, in the case of TL this equation becomes:

$$I_{TL} = -\frac{dn}{dt} = n\,s\,e^{-\frac{E}{k\,T}}. \tag{20}$$

Assuming a linear heating rate $\beta = dT/dt$, Eq. (20) becomes

$$I_{TL} = -\frac{dn}{dT} = \frac{n\,s}{\beta}\,e^{-\frac{E}{k\,T}}. \tag{21}$$

The solution of Eq. (21) is the well known TL equation by Randall and Wilkins (1945a, b) for first order kinetics:

$$I_{TL}(T) = \frac{n_0\,s}{\beta}\,e^{-\frac{E}{k\,T}}\,exp\left[-\frac{s}{\beta}\int_{T_0}^{T} e^{-\frac{E}{k\,T'}}dT'\right], \tag{22}$$

where n_0 is the initial value of the concentration of trapped electrons at $t = 0$, T_0 is the initial temperature and T' is a dummy integration variable representing temperature. The units of Eq. (22) are easily found to be $cm^{-3}\,K^{-1}$.

The OTOR model also leads to second order kinetics, at the boundary condition $A_n = A_m$. In this case Eq. (19) leads to following differential equation for second order kinetics:

$$I = -\frac{dn}{dt} = \frac{n^2}{N}\,p(t).$$

In the case of TL this equation yields:

$$I_{TL} = -\frac{dn}{dt} = \frac{n^2}{N}\,s\,e^{-\frac{E}{k\,T}}. \tag{23}$$

Assuming again a linear heating rate, $\beta = dT/dt$, Eq. (23) becomes

$$I_{TL} = -\frac{dn}{dT} = \frac{n^2}{N}\,\frac{s}{\beta}\,e^{-\frac{E}{k\,T}}. \tag{24}$$

The solution of Eq. (24) is the well known second order kinetics equation by Garlick and Gibson (1948):

$$I_{TL}(T) = \frac{n_0^2\,s}{\beta\,N}\,e^{-\frac{E}{k\,T}}\left[1 + \frac{n_0\,s}{\beta\,N}\int_{T_0}^{T} e^{-\frac{E}{k\,T'}}dT'\right]^{-2}, \tag{25}$$

where all variables have the same meaning as in the equation for first order kinetics. The units of Eq. (25) are also $cm^{-3}\,K^{-1}$.

The general analytical solution of Eq. (19) is studied in detail in the next section.

3.4. The first master equation: analytical solution of the OTOR model

The system of differential equations representing the OTOR model are described by Eqs. (5)–(7). These rate equations are coupled first-–order non-linear differential equations, which unfortunately were never solved in a closed form. Obtaining an approximate solution requires some simplifying assumptions, with the most important being the quasi-equilibrium (QE) assumption.

Kitis and Vlachos (2013) and later Lovedy Singh and Gartia (2013) were able to solve analytically the GOT Eq. (19). According to Kitis and Vlachos (2013) the GOT can be written in the form:

$$I = -\frac{dn}{dt} = p(t)\,\frac{n^2}{(N-n)\,R + n}, \tag{26}$$

where the dimensionless quantity

$$R = A_n/A_m, \tag{27}$$

is called the retrapping ratio.

Rearranging Eq. (26) and integrating we obtain:

$$N\,R\int_{n_0}^{n}\frac{dn}{n^2} + (1-R)\int_{n_0}^{n}\frac{dn}{n} = -\int_{t_0}^{t} p(t)\,dt. \tag{28}$$

After some simple algebra, we obtain the following expression

$$\frac{n_0}{n} + c\,ln\left(\frac{n_0}{n}\right) = 1 + \frac{n_0}{N\,R}\int_{t_0}^{t} p(t)\,dt, \tag{29}$$

where c is a constant defined as:

$$c = \frac{n_0}{N}\,\frac{1-R}{R}. \tag{30}$$

The form of Eq. (29) depends on the value of c given by Eq. (30). For $A_n < A_m$ or $R < 1$, this equation leads to $c > 0$. Physically in this case the retrapping coefficient is less than the recombination coefficient. Conversely, for $A_n > A_m$ or $R > 1$, this equation leads to

$c < 0$, and the retrapping coefficient is higher than the recombination coefficient. These two cases must be investigated separately.

3.4.1. The case where $c > 0$ or $R = A_n/A_m < 1$

In this case, Eq. (29) takes the form

$$\frac{n_0}{n\,c} + ln\left(\frac{n_0}{n\,c}\right) = \frac{1}{c} - ln(c) + \frac{n_0}{c\,N\,R}\int_{t_0}^{t} p(t)\,dt. \tag{31}$$

Eq. (31) is a transcendental equation of the form

$$y + lny = z, \tag{32}$$

where

$$y = \frac{n_0}{n\,c}, \tag{33}$$

$$z = \frac{1}{c} - ln(c) + \frac{n_0}{c\,N\,R}\int_{t_0}^{t} p(t)\,dt. \tag{34}$$

Eq. (32) extends from $-\infty$ to ∞ and has a unique solution in terms of the Lambert W-function, which is given by Corless et al. (1996) and Corless et al. (1997):

$$y = W\,[e^z]. \tag{35}$$

Taking into account the transformation from Eq. (33), we obtain the following solution for n:

$$n = \frac{N\,R}{1-R}\,W\,[e^z]^{-1}. \tag{36}$$

By substituting the value of n from Eq. (36) into Eq. (26) and applying simple algebra, the following general analytical expression is obtained, which describes TL, LM-OSL and CW-OSL signals:

$$I(t) = \frac{N\,R}{(1-R)^2}\,\frac{p(t)}{W\,[e^z] + W\,[e^z]^2}. \tag{37}$$

This is the desired analytical solution of the GOT Eq. (19), which represents the solution of the OTOR Eqs. (5)–(7) under the QE conditions. The analytical Eq. (37) is a master equation able to describe a wide variety of stimulated luminescence phenomena (Bos and Wallinga, 2009; Kitis et al., 2006a; Lawless and Lo, 2001), provided that they are described by the OTOR model. The only thing needed is to specialize the function $p(t)$ for the desired stimulated luminescence effect. In the following we will consider the cases of a single TL peak or a single LM-OSL peak, and also the decay curves of CW-OSL, IRSL and ITL which are described by functions with the same mathematical form.

The function z has the following forms for TL, LM-OSL and ITL,CW-OSL,IRSL processes:

$$z_{TL} = \frac{1}{c} - ln(c) + \frac{s}{(1-R)\,\beta}\int_{T_0}^{T} exp\left[-\frac{E}{k\,T}\right]dT, \tag{38}$$

$$z_{LM-OSL} = \frac{1}{c} - ln(c) + \frac{\lambda\,t^2}{2\,(1-R)}, \tag{39}$$

$$z_{CW-OSL} = \frac{1}{c} - ln(c) + \frac{\lambda\, t}{(1-R)}. \tag{40}$$

3.4.2. The case where $c < 0$ or $R = A_n/A_m > 1$

In this case the quantity $ln(c)$ will be a complex number. In order to overcome this we define $c = -|c|$, so that Eq. (29) then takes the form

$$\frac{n_0}{n\,|c|} - ln\left(\frac{n_0}{n\,|c|}\right) = \frac{1}{|c|} + ln(|c|) + \frac{n_0}{|c|\,N\,R}\int_{t_0}^{t} p(t)\,dt. \tag{41}$$

Eq. (41) is a transcendental equation of the form:

$$y - lny = z, \tag{42}$$

where

$$y = \frac{n_0}{n\,|c|} > 0, \tag{43}$$

$$z = \frac{1}{|c|} + ln(|c|) + \frac{n_0}{|c|\,N\,R}\int_{t_0}^{t} p(t)\,dt. \tag{44}$$

Eq. (42) is positive everywhere. In the limit $y \to 0$, the function $(y - lny) \to \infty$, while for $y \to \infty$, the function $(y - lny) \to \infty$. The function $y - lny$ has a minimum at $y = 1$. Therefore, for $z < 1$ Eq. (42) has no solution. For $z = 1$ the unique solution is $y = 1$.

Finally, for $z > 1$, there are two solutions corresponding to the two branches of the Lambert W-function, i.e.,

$$y_1 = -W[0, -e^{-z}], \tag{45}$$

$$y_2 = -W[-1, -e^{-z}]. \tag{46}$$

and the terms $\frac{1}{c} - lnc$ must be replaced by $\frac{1}{|c|} + ln|c|$. Taking into account Eqs. (45) and (46) and the transformations of Eq. (43), we obtain the following solution for n:

$$n = -\frac{N\,R}{|1-R|}\,W[k, -e^{-z}]^{-1}, \tag{47}$$

where $k = 0$, $k = -1$ refer to the first and second real branch of $W(z)$ respectively. By substituting the value of n from Eq. (47) into Eq. (26) and after some algebra, the following general analytical expression is obtained:

$$I(t) = \frac{N\,R}{(1-R)^2}\,\frac{p(t)}{W[k, -e^{-z}]^2 + W[k, -e^{-z}]}. \tag{48}$$

Kitis and Vlachos (2013) showed that only the $k = -1$ branch has physical meaning, and therefore, the final equation for the case when $c < 0$ is:

$$I(t) = \frac{N\,R}{(1-R)^2}\,\frac{p(t)}{W[-1, -e^{-z}] + W[-1, -e^{-z}]^2}. \tag{49}$$

The new Eq. (49) is similar to Eq. (37). The only difference is that the new Eq. (49) contains the second real branch of the Lambert W-function, instead of the principal $k = 0$ branch. Furthermore, some additional care is required regarding the values of z given by Eq. (44). Specifically, in the expressions of z given in Eqs (38)–(40), the term $\frac{1}{c} - lnc$ must be replaced by $\frac{1}{|c|} - ln|c|$ when using Eq. (49) for $R > 1$.

Summarizing, the analytical solution of the OTOR model is the following first master equation:

The first master equation (GOT/OTOR model)

$$I(t) = \frac{N\,R}{(1-R)^2}\,\frac{p(t)}{W[e^z] + W[e^z]^2} \quad \text{for } R = A_n/A_m < 1. \tag{50}$$

$$I(t) = \frac{N\,R}{(1-R)^2}\,\frac{p(t)}{W[-1, -e^{-z}] + W[-1, -e^{-z}]^2} \quad \text{for } R = A_n/A_m > 1. \tag{51}$$

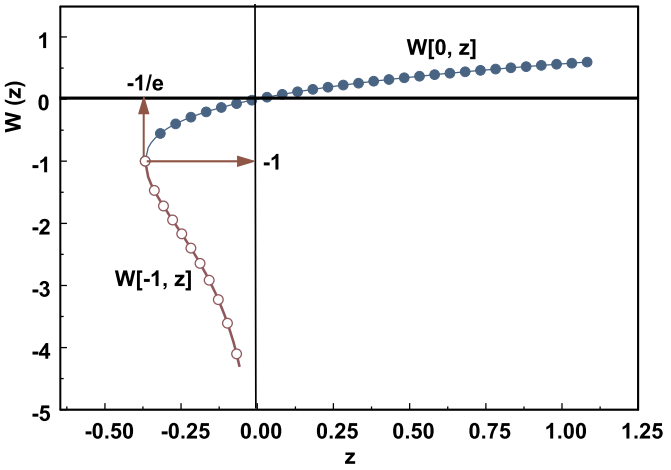

Fig. 3. The real branches of the Lambert W -function. The real branch $W[0, z]$ is defined for $-1/e \le z \le +\infty$ and is called the principal branch. The second branch $W[-1, z]$ is defined between $-1/e \le z \le 0$. The two branches have a common point at $(-1/e, -1)$, which belongs to both branches.

3.5. On the lambert W function

An extensive and comprehensive presentation of the Lambert W-function is given by Corless et al. (1996). In brief, the Lambert W-function $W(z)$ is defined as the inverse of the function $f(z) = ze^z$, which satisfies $W(z)e^{W(z)} = z$ for any complex number z.

The Lambert W-function is a multi-valued function displaying infinite complex branches and only two real branches, which are of interest in the present work. The two real branches of the Lambert W-function are shown in Fig. 3. The upper real branch (solid circles) is defined for $-\frac{1}{e} \le z \le \infty$ and it is denoted by $W[0, z]$ or $W_0[z]$ or simply $W[z]$. The lower real branch (open circles) is defined for $-\frac{1}{e} \le z \le 0$ and is denoted by W[-1,z] or $W_{-1}[z]$.

Corless et al. (1996), studied extensively the properties of the Lambert W-function and its applications. Several authors (Corless et al., 1997; Valluri et al., 2000; Boyd, 1998; Golicnik, 2012) presented important applications of the Lambert W-function in physics, whereas Barry et al. (2000) gave an extensive list of Lambert W-function applications in various research fields.

The application of the Lambert function $W(z)$ is quite complicated when one has to use analytical approximations for it (Kitis and Vlachos, 2013). However, due to its importance, the Lambert W-function has been implemented in various software packages as a built-in function. In these cases its application is very simple in software packages (for example MATHEMATICA, MATLAB, ORIGIN etc) which contain it as a built-in function, similar to any other transcendental function like sine, cosine etc.

3.6. Testing the first master equation against the system of differential equations in OTOR

Kitis and Vlachos (2013) tested the first master equation (Eqs. (50) and (51)), by comparing it with the numerical solution of the differential equation of the GOT model. An example for TL and LM-OSL simulated signals is shown in Fig. 4 for $R < 1$ using Eq. (50). Fig. 5 shows similar results for TL and LM-OSL simulated signals, obtained for $R > 1$ using Eq. (51).

The results of Figs. 4 and 5 show that the analytical first master equation represents very accurately the results of the GOT model.

4. The IMTS and NMTS models: second and third master equations

This section presents the more general interactive multi-trap system

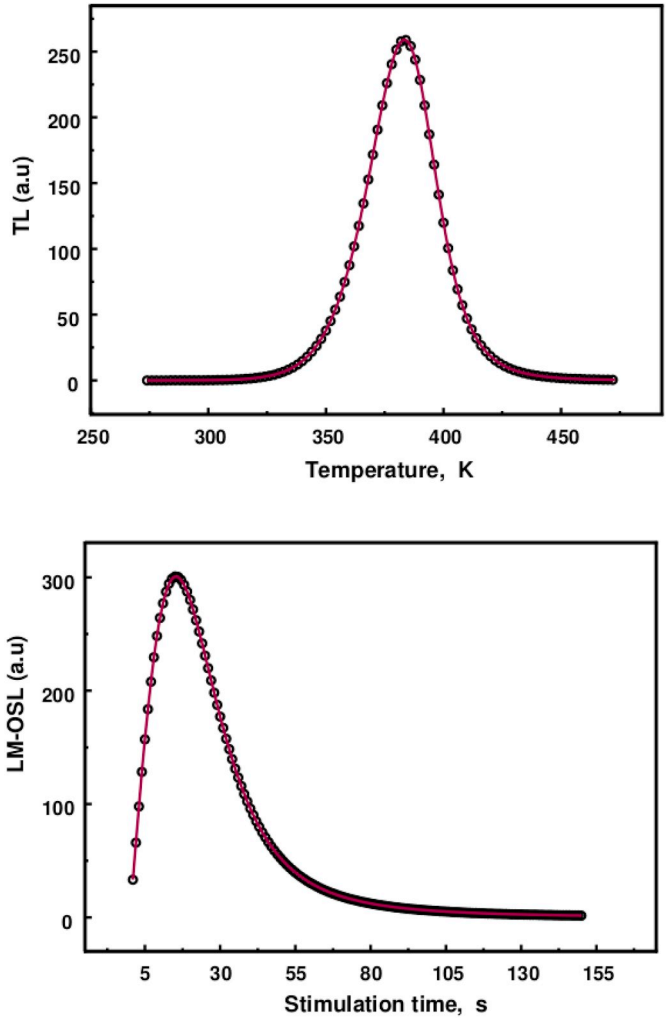

Fig. 4. Characteristic TL, LM-OSL curves for $A_n < A_m$(i.e $c > 0$). In all cases, the open circles correspond to the numerical solution of the OTOR model (Eqs (5)–(7)), and the solid lines correspond to the evaluation using the first master equations. The parameter values used were $N = n_0 = 10^{10} cm^{-3}$, $A_m = 10^{-7} cm^3 s^{-1}$ and $A_n = 4.6 \times 10^{-8} cm^3 s^{-1}$ for all cases. In the case of TL the activation energy was $E = 1\ eV$, $s = 10^{12} s^{-1}$ and the heating rate was $\beta = 1K/s$. The parameter value α was 0.003 s^{-1} for LM-OSL. From Kitis and Vlachos (2013).

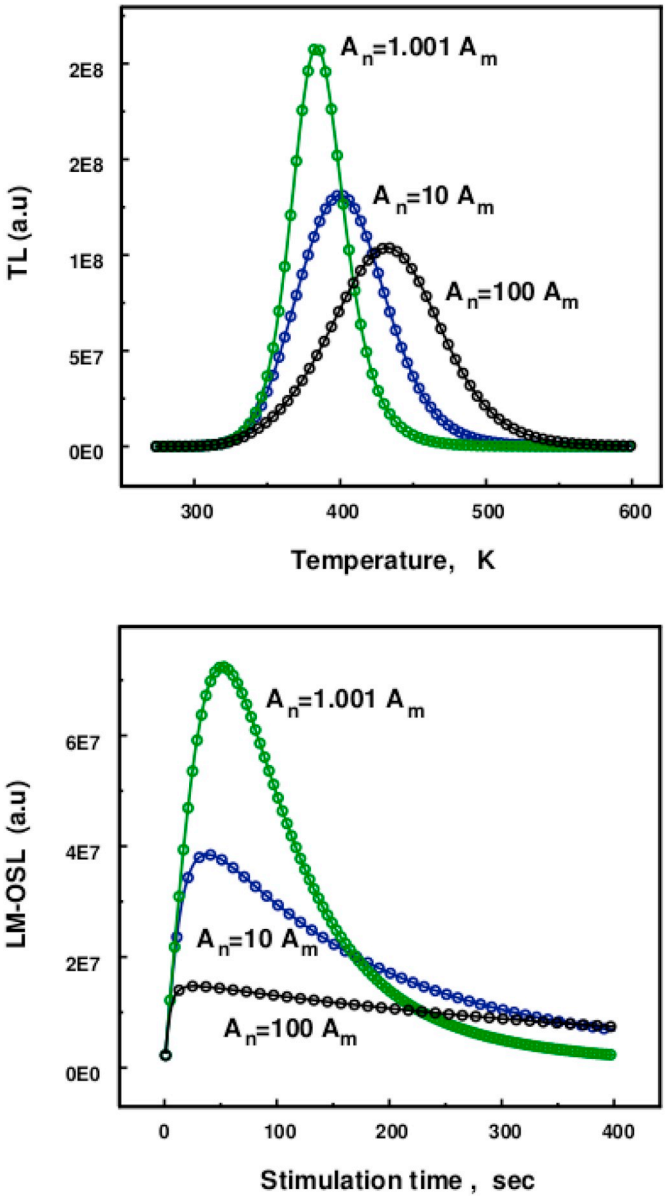

Fig. 5. Characteristic TL and LM-OSL curves for three cases of $A_n > A_m$(i.e. $c < 0$) with $A_m = 10^{-9} (cm^3 s^{-1})$. The open circles correspond to the numerical solution of the OTOR model (Eqs (5)–(7)) and the solid lines correspond to the evaluation using the first master equations. All other parameter values are the same as the values used in 4. From Kitis and Vlachos (2013).

model (IMTS), and its more restricted version known as the non-interacting multi trap system (NMTS). Under special physical assumptions, the NMTS model is shown to lead to the mixed-order kinetics model (MOK), which is a linear combination of the equations for first and second order kinetics. The analytical solutions of the MOK and NMTS models constitute the second and third master equations presented in this paper.

An attempt to cover the gap between first and second order kinetics was made by Chen et al. (1981) who introduced the mixed order kinetics (MOK) for TL. Later on introduced the MOK model for OSL.

4.1. The IMTS, NMTS and MOK models

In the previous section we presented the OTOR model as a basic luminescence model, whose analytical solution is the first master equation. The more complicated interactive multi-trap system model (IMTS) is shown schematically in the energy band model of Fig. 6.

The system of differential equations describing the traffic of charged carriers during the irradiation stage in the IMTS model are:

$$\frac{dn_i}{dt} = -n_i\, p(t) + A_i\,(N_i - n_i)\, n_c \qquad i = 1..n, \tag{52}$$

$$\frac{dn_d}{dt} = A_d (N_d - n_d)\, n_c, \tag{53}$$

$$\frac{dm}{dt} = A_h\,(M - m)\, n_v - A_m\, m\, n_c, \tag{54}$$

$$\frac{dn_v}{dt} = R - A_h\,(M - m)\, n_v, \tag{55}$$

$$\frac{dn_c}{dt} = R - \sum_i \frac{dn_i}{dt} - \frac{dn_d}{dt} - A_m\, m\, n_c, \tag{56}$$

where the index $i = 1..n$ stands for the electron traps, $N_i\ (cm^{-3})$ is the concentration of available electron traps, $n_i\ (cm^{-3})$ the concentration of trapped electrons, $M\ (cm^{-3})$ is the concentration of available luminescence centers, $m_i\ (cm^{-3})$ the concentration of trapped holes.

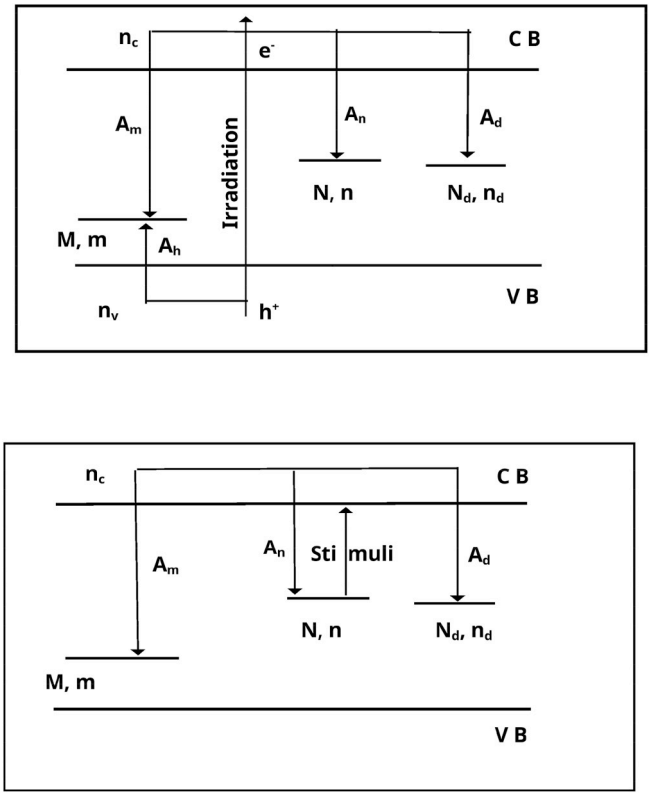

Fig. 6. The general phenomenological interactive multitrap trap (IMTS) model, describing stimulated luminescence effects, for (a) the Irradiation stage and (b) for the thermal or optical stimulation stage.

N_d, n_d (cm^{-3}) are the concentrations of available and occupied traps respectively in a thermally disconnected deep trap (TDDT), n_c (cm^{-3}) and n_v (cm^{-3}) are the concentrations of electrons in the conduction and holes in the valence band, A_i $(cm^3\ s^{-1})$ are the trapping coefficients in electron traps n_i, A_m $(cm^3\ s^{-1})$ is the recombination coefficient, A_h $(cm^3\ s^{-1})$ the trapping coefficient of holes in luminescence centers, A_d $(cm^3\ s^{-1})$ the trapping probability in TDDT, β (K/s) the heating rate and R is the rate of production of ion (electron-holes) pairs (i.p) per second and per unit volume, which is proportional to the dose rate. A detailed listing of the parameters in the IMTS model is given in Table 1.

In the above model all traps having the index i can trap and release electrons by excitation, and they are referred to as active traps. On the other hand, the trap with index d can only trap electrons but thermal stimulation is not allowed, so these traps are called thermally disconnected deep traps (TDDT).

During the heating stage and for a single active trap these equations become:

$$\frac{dn_1}{dt} = -n_1\, p(t) + A_n\,(N_1 - n_1)\, n_c, \tag{57}$$

$$\frac{dn_d}{dt} = A_d (N_d - n_d)\, n_c, \tag{58}$$

$$\frac{dm}{dt} = \frac{dn_1}{dt} + \frac{dn_d}{dt} + \frac{dn_c}{dt}, \tag{59}$$

$$I(t) = -\frac{dm}{dt} = A_m\, m\, n_c, \tag{60}$$

where $p(t)$ depends again on the experimental stimulation mode.

The concentration of holes m in the recombination centers (RC) is equal to:

$$m = n_1 + n_c + n_d, \tag{61}$$

so that the charge balance of the system is maintained.

When during the irradiation stage the TDDT (N_d) becomes saturated i.e. when $n_{d0} = N_d$, this trap cannot capture free carriers from the conduction band during the stimulation stage. This is known as the non-interactive multi-trap system (NMTS) limit of the IMTS model.

As in the case of the OTOR model, it is possible to arrive at an analytical expression for the NMTS model, by using the QE conditions. In this model the QE is expressed by the relation:

$$\frac{dn_c}{dt} \ll \frac{dn_1}{dt},\ \frac{dn_d}{dt},\ \frac{dm}{dt}. \tag{62}$$

Since the TDDT in the NMTS model is saturated, we have $dn_d/dt = 0$. By proceeding as in the GOT equation, Eq. (59) can be solved with respect to n_c, and then can be replaced in Eq. (60) to obtain:

$$I = p(t)\, n_1 \frac{(n_1 + N_d)\, A_m}{(N_1 - n_1)\, A_n + (n_1 + N_d)\, A_m}. \tag{63}$$

In the case of slow re-trapping $(N_1 - n_1)A_n \ll (n_1 + N_d)A_m$, and Eq. (63) leads directly to the first-order kinetics expression.

Alternatively, in the case of fast re-trapping, the condition $(N_1 - n_1)A_m \gg (n_1 + N_d)A_n$, along with $n_1 \ll N_1$ for low irradiation doses, leads to the following expression for the stimulated luminescence intensity:

$$I = \frac{A_m}{N_1\, A_n}\, p(t)\, n_1\, (n_1 + N_d). \tag{64}$$

For the special case of $A_n = A_m$, Eq. (63) becomes:

$$I = \frac{1}{N_1 + N_d}\, p(t)\, n_1\, (n_1 + N_d). \tag{65}$$

Both Eqs. (64) and (65) can be presented in the form

$$I = g\, p(t)\, n_1\, (n_1 + N_d), \tag{66}$$

with $g = A_m/(N_1\, A_m)$ or $g = 1/(N_1 + N_d)$ correspondingly. This is the differential equation for the MOK model, which is the sum of the two terms $g\, p(t)\, n_1\, N$ and $g\, p(t)\, n_1^2$, corresponding to first and second order kinetics respectively (Chen et al., 1981). In the next subsection we present the analytical solution of Eq. (66).

4.2. The second master equation: analytical solution of the MOK model

In order to obtain an analytical expression for the MOK model, we use $I = -dm/dt \approx -dn_1/dt$ and write Eq. (66) in the form:

$$-\frac{dn_1}{dt} = g\, p(t)\, n_1\, (n_1 + N_d)\,. \tag{67}$$

After integration and some algebra, the following expression is obtained

$$ln\left(\frac{n_1 + N_d}{n_1}\,\frac{n_{10}}{n_{10} + N_d}\right) = g\, N_d \int_0^t p(t)\, dt, \tag{68}$$

where n_{10} is the initial concentration of trapped electrons at $t = 0$.

At this point we define the mixed order parameters α (Chen et al., 1981) as:

$$\alpha = \frac{n_{10}}{n_{10} + N_d}. \tag{69}$$

From Eq. (68) it is found that

$$n_1(t) = \frac{\alpha\, N_d}{F(t) - \alpha}, \tag{70}$$

with $F(t)$ given by:

$$F(t) = exp\left(g\, N_d \int_0^t p(t)\, dt\right). \tag{71}$$

By inserting $n_1(t)$ from Eq. (70) in Eq. (67), the following expression describing the intensity of the stimulation phenomena in the MOK

model is obtained:

The second master equation (MOK model)

$$I(t) = g\, N_d^2\, \frac{\alpha\, p(t)\, F(t)}{[F(t) - \alpha]^2}. \tag{72}$$

This second master equation joins together several previous expressions previously available in the literature for MOK in TL (Chen et al., 1981), and also for OSL (Kitis et al., 2009).

Eq. (72) is again a general equation containing the function $p(t)$ which describes the various experimental luminescence modes. The function $F(t)$ in Eq. (72) has the following forms for TL, LM-OSL and ITL, CW-OSL, IRSL processes:

$$F_{TL}(t) = exp\left(g\, N_d\, \frac{s}{\beta} \int_{T_0}^{T} e^{-\frac{E}{k\,T}}\, dT\right), \tag{73}$$

$$F_{LM-OSL}(t) = exp\left(g\, N_d\, \frac{\lambda\, t^2}{2P}\right), \tag{74}$$

$$F_{PID}(t) = exp(g\, N_d\, \lambda\, t). \tag{75}$$

As discussed previously, Eq. (75) also applies for CW-OSL and CW-IRSL signals, with the appropriate value of the excitation constant λ. The exponential integral of Eq. (73) is discussed in section 9.

The second master Eq. (72) has been applied successfully to simulated luminescence signals, as well as to a wide variety of experimental data over the past 50 years (Yossian and Horowitz, 1997; Kitis and Gomez Ros, 1999; Gomez Ros and Kitis, 2002).

4.3. The third master equation: analytical solution of the NMTS model

The analytical expression of the luminescence intensity in the NMTS model is (Sadek et al., 2015b):

$$I(t) = p(t)\, n_1 \frac{m\, A_m}{(N_1 - n_1)\, A_n + m\, A_m}, \tag{76}$$

where $p(t)$ represents the stimulation modes as before. From the charge neutrality condition:

$$m(t) = n_1(t) + N_d + n_c(t). \tag{77}$$

Within the QE approximation, it is assumed that $n_c \ll n_1 + N_d$, so that Eq. (77) becomes:

$$m(t) \cong n_1(t) + N_d. \tag{78}$$

By using Eq. (78), Eq. (76) can be now written as a differential equation for the concentration $n_1(t)$ (Sadek et al., 2015b) as:

$$I(t) = -\frac{dn_1}{dt} = p(t)\, \frac{(n_1 + N_d)\, n_1}{(N_1 - n_1)\, R + (n_1 + N_d)}. \tag{79}$$

Sadek et al. (2015b) introduced the following dimensionless function:

$$\varphi_{eff}(t) = \frac{n_1(t)}{m(t)} = \frac{n_1(t)}{n_1(t) + N_d}. \tag{80}$$

This expression is mathematically similar to the mixed order parameter α defined in section 4 as in Eq. (69):

$$\alpha = \frac{n_{10}}{n_{10} + N_d}.$$

The difference is that in the case of the NMTS model, this parameter $\varphi_{eff}(t)$ is time dependent. It is obvious that the values of the NMTS parameter $\varphi_{eff}(t)$ are between 0 and 1 ($0 < \varphi_{eff} < 1$), similar to the α parameter in the MOK model.

Following along the derivation method of Kitis and Vlachos (2013) and section 3.4, the general Eq. (76) after some algebra takes the form of the following transcendental equation:

$$y_1 + ln(y_1) = z_1, \tag{81}$$

where

$$y_1 = \frac{m_0}{m\, \varepsilon}, \tag{82}$$

$$\varepsilon = \frac{m_0(1 - \varphi_{eff}\, R)}{N_1\, R}, \tag{83}$$

$$z_1 = \frac{1}{\varepsilon} - ln(\varepsilon) + \frac{\varphi_{eff}}{1 - \varphi_{eff}\, R} \int_0^t p(t)\, dt. \tag{84}$$

As in the case of OTOR in section 3.4, we have in principle two different cases, depending on whether the retrapping ratio $R = A_n/A_m$ is $R < 1$, or $R > 1$.

In the case of $R < 1$, one has always $1 - \varphi_{eff}\, R > 0$, so the solution of Eq. (81) is written in terms of the first real branch of the Lambert W function as (Corless et al., 1996):

$$m = \frac{m_0}{\varepsilon}\, \frac{1}{W[e^{z_1}]}. \tag{85}$$

Replacing this value of m in Eq. (79) we obtain:

$$I(t) = \frac{N_1\, R\, \varphi_{eff}}{(1 - \varphi_{eff}\, R)^2} \cdot \frac{p(t)}{W_0[e^{z_1}] + W_0[e^{z_1}]^2}. \tag{86}$$

In the case of $R > 1$ we again have two possible situations. If $(1 - \varphi_{eff}\, R) > 0$ then this case is equivalent to the case with $R < 1$ discussed above. However, if $(1 - \varphi_{eff}\, R) < 0$, then according to Kitis and Vlachos (2013), we set $\varepsilon = -|\varepsilon|$ and the solution becomes:

$$y_1 - lny_1 = z_2, \tag{87}$$

$$z_2 = \frac{1}{|\varepsilon|} + ln(|\varepsilon|) + \frac{\varphi_{eff}}{|1 - \varphi_{eff}\, R|} \int_0^t p(t)\, dt. \tag{88}$$

The solution of Eq. (87) is given in terms of the second real branch of the Lambert W function (Corless et al., 1996, 1997), i.e.

$$m = \frac{-m_0}{\varepsilon}\, \frac{1}{W[-1,\ -e^{-z_1}]}. \tag{89}$$

Replacing in Eq. (79) we obtain

$$I(t) = \frac{N_1\, R\, \varphi_{eff}}{(1 - \varphi_{eff}\, R)^2}\, \frac{p(t)}{W[-1,\ -e^{-z_2}] + W[-1,\ -e^{-z_2}]^2}. \tag{90}$$

Eqs (86) and (90) are in a one-to-one correspondence with Eqs. (37) and (49). Therefore, these equations are also master equations, each one representing a large family of stimulated luminescence phenomena.

The third master equation (NMTS model)

$$I(t) = \frac{N_1\, R\, \varphi_{eff}}{(1 - \varphi_{eff}\, R)^2}\, \frac{p(t)}{W_0[e^{z_1}] + W_0[e^{z_1}]^2}. \quad \text{for } R < 1 \tag{91}$$

$$I(t) = \frac{N_1\, R\, \varphi_{eff}}{(1 - \varphi_{eff}\, R)^2}\, \frac{p(t)}{W[-1,\ -e^{-z_2}] + W[-1,\ -e^{-z_2}]^2}. \quad \text{for } R > 1 \tag{92}$$

As in the case of the OTOR model, what is needed is to select the stimulation mode $p(t)$ in order to construct the respective z_1, z_2 function given by Eqs. (84) and (88). Sadek et al. (2015b) tested the third master equation against the numerical solution of the differential equations in NMTS, and found very good agreement between the two approaches.

5. The simple localized transition model (SLT): fourth master equation

Localized transition luminescence models (LTMs) are used to describe behaviors of luminescence signals in a wide variety of materials. Since the original work of Halperin and Braner (1960), many variations of these models have been developed. All of these are based on the assumption that the recombination probability between the excited

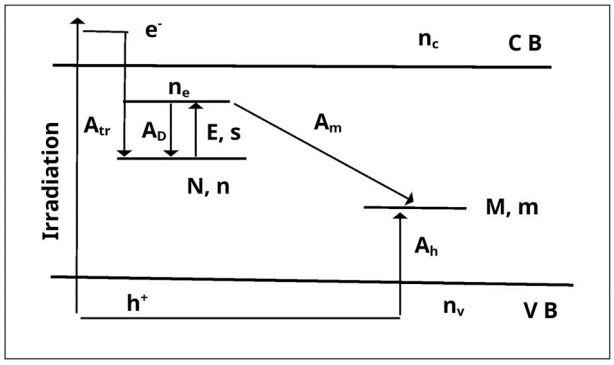

Fig. 7. Energy band diagram for the simple localized transition model (SLT). From Kitis and Pagonis (2018)).

state of a trap and the recombination center is constant (Bull, 1989; Templer, 1986; Mandowski, 2005; Pagonis et al., 2017; Pagonis, 2005). The LTMs have been reviewed for example in the luminescence books by Bøtter-Jensen et al. (2003), Chen and McKeever (1997) and Chen and Pagonis (2011).

5.1. The simple localized transition (SLT) model

As was discussed above, the case of localized transition with a stable recombination probability is the basis of many models published during the last fifty years. The energy band diagram for the localized transition model used by Kitis and Pagonis (2018) is shown in Fig. 7. During irradiation, electrons and holes are created in the conduction and valence bands, and are subsequently trapped into the ground state of the trap and the recombination center correspondingly. These transitions are indicated by A_{tr} and A_h in Fig. 7. During the heating stage, electrons are raised into the excited state of the electron trap, from which they can either recombine at the recombination center (transition A_m), or they can be de-excited back into the ground state (transition A_D). As mentioned above, in this model the conduction and valence bands participate in the kinetics only during the irradiation stage.

The differential equations governing the traffic of free carriers during both the irradiation and heating stage are:

$$\frac{dT}{dt} = \beta \quad \text{or} \quad \frac{dT}{dt} = 0, \tag{93}$$

$$\frac{dn}{dt} = -n\,p(t) + A_D\,n_e + A_{tr}(N-n)n_c, \tag{94}$$

$$\frac{dm}{dt} = A_h\,(M-m)\,n_v - A_m\,m\,n_e, \tag{95}$$

$$\frac{dn_e}{dt} = n\,p(t) - A_D\,n_e - A_m\,m\,n_e, \tag{96}$$

$$\frac{dn_v}{dt} = X - A_h\,(M-m)\,n_v, \tag{97}$$

$$\frac{dn_c}{dt} = X - A_{tr}\,(N-n)\,n_c. \tag{98}$$

The symbols in the model are: $N\ (cm^{-3})$ is the concentration of available electron traps, $n\ (cm^{-3})$ the concentration of trapped electrons, $M\ (cm^{-3})$ is the concentration of available luminescence centers, $m\ (cm^{-3})$ is the concentration of trapped holes. $n_c\ (cm^{-3})$ and $n_v\ (cm^{-3})$ are the concentrations of electrons in the conduction band and holes in the valence band respectively. $A_{tr}\ (cm^3\,s^{-1})$ is the trapping coefficient in electron traps and $A_h\ (cm^3\,s^{-1})$ is the trapping coefficient of holes in luminescence centers. $E\ (eV)$ is the thermal activation energy, $s\ (s^{-1})$ is the frequency factor and k the Boltzmann constant, $\beta\ (K/s)$ is the heating rate and X is the rate of production of ion pairs per second $(i.\ p/s)$, which is proportional to the dose rate.

n_e is the concentration of electrons in the excited state of the trap, $p(t)$ is the rate of excitation from the ground state energy level of the trap into the excited state, from which the electron can either recombine with a recombination coefficient $A_m\ (cm^3\,s^{-1})$, or alternatively it can de-excite back into the ground state with a de-excitation coefficient $A_D\ (s^{-1})$. The rate of excitation $p(t)$ depends on the type of experiment (LM-OSL, CW-OSL etc), and is of course different for thermal and optical excitation. For example, in TL experiments the rate of thermal excitation is $p(t) = s\,exp\left(-\frac{E}{k\,T}\right)$, while in CW-OSL experiments the rate of optical excitation is constant $\lambda\ (s^{-1})$, which depends on the optical cross section of the trap and on the intensity of the stimulating light source. In the case of LM-OSL experiments, the rate of excitation is varied linearly with time according to $p(t) = \lambda t/P$, where $\lambda\ (s^{-1})$ is the rate of optical excitation and P is the total stimulation time during the LM-OSL experiment. The three stages are simulated with the above system of equations by using $\beta = 0$ for the irradiation stage, $\beta = 0$ and $X = 0$ for the relaxation stage, and $X = 0$, $A_{tr} = 0$, $A_h = 0$ for the heating stage.

An important point to note in these equations is that the recombination rate is written here in the form $-A_m\,m\,n_e$, where A_m is considered independent of the distance between the traps and the recombination center, in agreement with the original model of Halperin and Braner (1960). In the later versions of the model by Chen and Kirsh (1981) and Bull (1989), this term is written as $-\gamma\,n_e$, where γ is a constant with dimensions of s^{-1}. In addition, the de-excitation term in the above equations is written here as $-A_D\,n_e$, while in these previous publications it is written as $-s\,n_e$, based on the assumption that the principle of detailed balance is valid for the model (i.e. $A_D = s$).

According to the principle of detailed balance (PDB), the de-excitation rate coefficient A_D must be equal to the frequency factor s. However, the PDB has been derived for a system in thermal equilibrium (Chen and Pagonis, 2011, their Chapter 2), and experimental studies have raised the question whether it is applicable for systems in non-thermal equilibrium (Lloyd and Pake, 1954). Furthermore, theoretical work has shown that the PDB applies only to cyclic systems (Klein, 1955; Thomsen, 1953). As a consequence of these theoretical studies, the PDB will not be applicable in a multiple level model such as the localized model in Fig. 7.

Kitis and Pagonis (2018) assumed that the PDB does not apply, and studied the consequences of this assumption on the model. In addition, these authors used the original version of the model as written by Halperin and Braner (1960), by writing the recombination rate in the form $-A_m\,m\,n_e$.

The above system of differential equations was solved analytically by Kitis and Pagonis (2018) under the QE assumptions, in order to obtain analytical expressions for stimulated luminescence signals in the localized transition model. This is described in the next subsection.

5.2. The fourth master equation: analytical solution of the SLT model

By considering the heating stage for which it is $X = 0$ and $A_h = 0$, and assuming that the system is in a quasi-equilibrium state (Chen and McKeever, 1997), we set $dn_e/dt = 0$ in Eq. (96), to obtain the concentration of electrons in the excited state n_e :

$$n_e = \frac{n\,p(t)}{A_D + A_m\,m}. \tag{99}$$

By substituting this value of n_e into Eq. (95):

$$\frac{dm}{dt} = -A_m\,m\,n_e = -p(t)\,\frac{n\,m\,A_m}{A_D + A_m\,m}. \tag{100}$$

We now make the common assumption that only a few electrons are in the excited state at any given moment, i.e. $n_e \ll n$ and therefore from the conservation of charge $m = n + n_e$ one obtains $m \approx n$. With this approximation, the luminescence intensity becomes:

$$I_{LOC} = -\frac{dn}{dt} = p(t)\,\frac{n^2}{r+n}, \tag{101}$$

where

$$r = \frac{A_D}{A_m}. \tag{102}$$

Eq. (101) has the exact same mathematical form as the following general one trap (GOT) equation of the OTOR model (see sections 3.4 and 4.3):

$$I_{DEL} = p(t)\,\frac{n^2}{NR + n(1-R)}. \tag{103}$$

From this point on, one follows closely the method of Kitis and Vlachos (2013), and Eq. (101) can be integrated. After some extended but simple algebra a transcendental equation exactly similar to Eqs. (32) and (42) in section 3.4, and Eqs. (81) and (87) in section 4.3 is obtained, which is solved in terms of the Lambert W function. The analytical solutions obtained for the localized model are Kitis and Pagonis (2018):

The fourth master equation (SLT model)

$$I_{LOC}(t) = p(t)\,\frac{r}{W[0,e^z] + W[0,e^z]^2}. \tag{104}$$

$$z_{LOC} = \frac{r}{n_0} - ln\left[\frac{n_0}{r}\right] + \int_{t_0}^{t} p(t)dt. \tag{105}$$

Eqs. (104) and (105) are master equations, similar to those obtained by Kitis and Vlachos (2013) for the OTOR model, and by Kitis and Pagonis (2013) for the localized tunneling recombination model of Jain et al. (2012).

The function z in this master equation has the following specialized forms for the various luminescence excitation modes:

$$z_{LOC-TL} = \frac{r}{n_0} - ln\left[\frac{n_0}{r}\right] + s\int_{T_0}^{T} exp\left(-\frac{E}{k\,T}\right)dT, \tag{106}$$

$$z_{LOC-LMOSL} = \frac{r}{n_0} - ln\left[\frac{n_0}{r}\right] + \frac{\lambda\,t^2}{2}, \tag{107}$$

$$z_{LOC-CWOSL,ITL,IRSL} = \frac{r}{n_0} - ln\left[\frac{n_0}{r}\right] + \lambda\,t. \tag{108}$$

It is important to emphasize that the r ratio in Eq. (102) is not a dimensionless quantity and has units of cm^{-3}, whereas by contrast, the parameter R in Eq. (27) is a dimensionless quantity expressing the ratio of the retrapping and recombination coefficients in the OTOR model (Kitis and Vlachos, 2013). Note that Halperin and Braner (1960) assumed that the principle of detailed balance holds, so that $r = s/A_m$ in their model. Here, r is used in the more general form of Eq. (102).

There is an additional important difference between the solutions of localized and delocalized transitions. In the case of the *delocalized* model the solution is based on *both* real branches of the Lambert W function, due to the presence of the term $(1-R)$ in denominator and the logarithmic argument in Eq. (105). On the other hand, in the case of the *localized* model, the solution in Eq. (104) is based *only* on the first real branch of the Lambert W function, for any value of r.

Kitis and Pagonis (2018) tested the fourth master equation Eq. (104), by comparing it with the numerical solution of the differential equation of the SLT model. An example for simulated TL signals is shown in Fig. 8a and b, showing that the analytical fourth master equation represents very accurately the results of the SLT model.

6. The tunneling localized transition (TLT) model: fifth master equation

Recent experimental and modeling studies reveal a time dependent localized tunneling/recombination probability. Of major interest is the

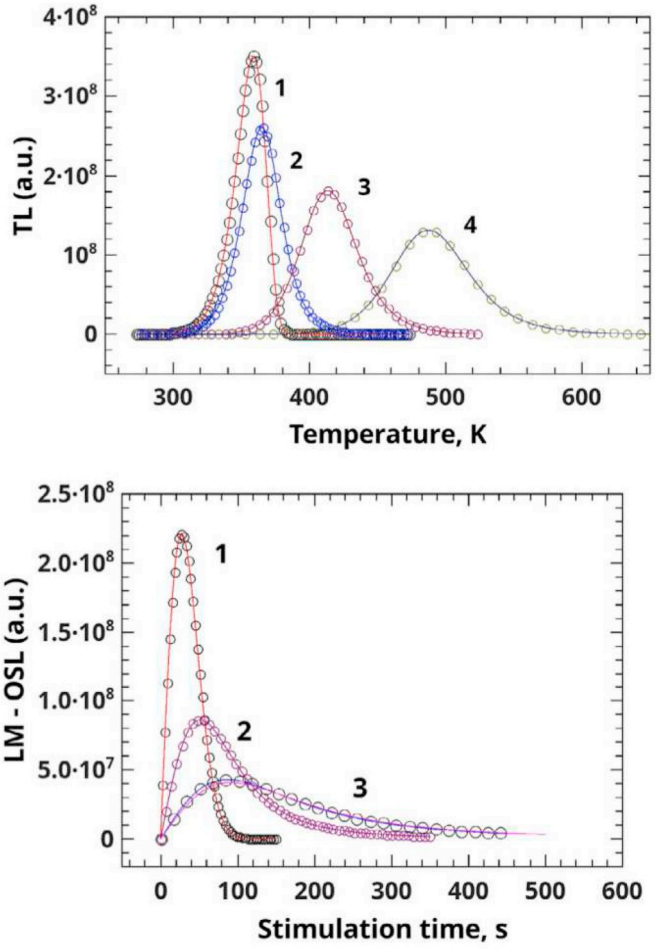

Fig. 8. (a) Comparison between peaks derived by numerical solution of differential equations (open circles), with numerical evaluation from the analytical solution based on Lambert W function (solid lines), for $A_D = 10^{-7}$, 10^5 and $10^7\ s^{-1}$. (b) Comparison of LM-OSL peaks derived by numerical solution of differential equations (open circles), with the analytical solution based on Lambert W function (solid lines) for (1) $\lambda = 0.2\ s^{-1}$ and $A_D = 10^{-7} - 10^0\ s^{-1}$, (2) $\lambda = 2\ s^{-1}$ and $A_D = 10^3\ s^{-1}$, (3) $\lambda = 4\ s^{-1}$ and $A_D = 10^5\ s^{-1}$. (from Kitis and Pagonis (2018)).

"anomalous fading" of luminescence signal observed mainly in feldspar samples, because these material are very important in dating studies (Wintle, 1977). In most of these studies it is suggested that the anomalous fading effect is due to quantum mechanical tunneling from the ground state of the trap to the luminescence center (Visocekas, 1985, 1988; Visocekas et al., 1994).

A very important development in this area is the general kinetic model by Jain et al. (2012), which quantifies localized recombination within randomly distributed donor-acceptor pairs. The energy band model is shown in Fig. 9. The recombination takes place via the excited stage of the donor, with the nearest neighbor randomly distributed acceptor. Jain et al. (2012) presented the model in two forms. In the first exact version of the model, the concentrations of trapped electrons evolve in both space and time, while in the second approximate version of the model the concentrations evolve only in time.

In the next two subsections, we will look at these two versions of this model. First, we look at the more general version of the model, which requires numerical integration of the differential equations. Second, we look at the analytical equations developed by Kitis and Pagonis (2013), which are applicable for freshly irradiated samples.

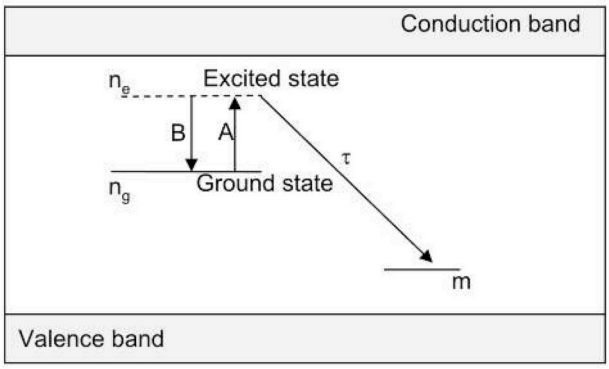

Fig. 9. The energy band model for localized recombination processes. Electrons are excited from the ground state (n_g) into the excited state (n_e) of the electron trapping center, at a rate A. From the excited state they can either tunnel to the nearest recombination center at the rate $1/\tau$, or relax back to the ground state of the trap at the rate B. In the exact model the tunneling lifetime is a function of the donor - acceptor separation distance r_0 , while in the semi-analytical model there exists a critical lifetime τ_c for the entire crystal. The concentrations n_g and n_e are expressed as a function of both distance and time in the exact model, while they are only a function of time in the semi-analytical model.

6.1. The general TLT model of Jain et al. (2012)

The equations for the model by Jain et al. (2012) are:

$$\frac{dn_g}{dt} = -p(t)\, n_g + B\, n_e, \tag{109}$$

$$\frac{dn_e}{dt} = p(t)\, n_g - B\, n_e - \frac{3\, n_e\, \rho'^{1/3}}{\tau_c}\, z \left(ln\, \frac{n_0}{n}\right)^{2/3}, \tag{110}$$

$$-\frac{dm}{dt} = \frac{3\, n_e\, \rho'^{1/3}}{\tau_c}\, z \left(ln\, \frac{n_0}{n}\right)^{2/3}, \tag{111}$$

with

$$\tau_c = s^{-1}\, exp\left[\left(\frac{1}{\rho'}\, ln\frac{n_0}{n}\right)^{1/3}\right]. \tag{112}$$

Symbol Units Physical meaning n_g (cm^{-3}) is the instantaneous concentration of electrons (donors) in the ground state, n_e (cm^{-3}) is the instantaneous concentration of electrons (donors) in the excited state, ρ' is the dimensionless number density of acceptors, τ_c (s^{-1}) is the critical tunneling lifetime, $z = 1.8$ is a dimensionless constant introduced in the model. B (s^{-1}) is the relaxation rate from the excited into the ground state. A detailed listing of the parameters in the model is given in Table 2.

The above general system of equations leads to an analytical solution by using specific physical assumptions, and this is described in the next subsection.

6.2. The fifth master equation: analytical solution of the approximate TLT model

Kitis and Pagonis (2013) derived an analytical equation from the approximate model of Jain et al. (2012). The approximate version of the model is based on the assumption that at any time t, the concentration of electrons in the excited state (n_e) is many orders of magnitude smaller than the corresponding concentration of electrons in the ground state (n_g) Furthermore, the relaxation process of the excited states is considered to be much faster than the time scales of TL and OSL experiments. Therefore, one can model the excited state in the quasi-steady approximation. More specifically, the time scale for electronic relaxation processes involving the excited states (corresponding to the term dn_e/dt in Eq. (110)) is of order of *ns* or *ms*. On the other hand, the time scale for TL processes is of the order of *ms* or *s* (corresponding to the luminescence term $3\,\rho'^{1/3}/\tau_c\, z\, (ln\, n_o/n)^{2/3}$ in Eq. (110)). Based on these assumptions, Kitis and Pagonis (2013) used the approximation:

$$\frac{1}{n_e}\frac{dn_e}{dt} \lll \left[B + z\, \frac{3\,\rho'^{1/3}}{\tau_c}\left(ln\frac{n_0}{n}\right)^{2/3}\right]. \tag{113}$$

Typical values of B are in the range of $10^6 - 10^{12} s^{-1}$ or higher, so these quasi-state assumptions are likely to be very accurate.

Taking into account Eq. (113), Eq. (110) yields:

$$n_e = \frac{p(t)\, n_g}{B + z\, (3\,\rho'^{1/3}/\tau_c)\, ln(n_o/n)^{2/3}}. \tag{114}$$

Substituting Eq. (114) into Eq. (109) we obtain

$$\frac{dn_g}{dt} = \frac{-p(t)\, n_g\, z\, (3\,\rho'^{1/3}/B\,\tau_c)\, ln\left(\frac{n_0}{n}\right)^{2/3}}{1 + z\, (3\,\rho'^{1/3}/B\,\tau_c)\, ln\left(\frac{n_0}{n}\right)^{2/3}} \simeq -p(t)\, n_g\, z\, \frac{3\,\rho'^{1/3}}{B\,\tau_c}\left(ln\frac{n_0}{n}\right)^{2/3}, \tag{115}$$

where it was assumed that for typical values of the parameters, the functional part of the denominator is much smaller than unity,

The derivative dn_g/dt of Eq. (115) represents the luminescence intensity as $I(t) = -dm/dt \approx -dn_g/dt$, since $m = (n_g + n_e) + N$ and $n_e \lll n_g$.

Kitis and Pagonis (2013) substituted Eq. (112) into Eq. (115) and obtained the following analytical solution for the luminescence intensity, by taking into account that $n = n_e + n_g \approx n_g$ and after some extended algebra:

The fifth master equation (Tunneling model)

$$I(t) = 3\, n_0\, \rho'\, z\, p(t)\, F(t)^2\, e^{-F(t)}\, e^{-\rho'(F(t))^3}. \tag{116}$$

$$F(t) = ln\left(1 + z\, \int_0^t p(t)\, dt\right). \tag{117}$$

Eq. (116) along with Eq. (117), constitute the fifth master equation.

The function $F(t)$ takes the following form for the various stimulated luminescence phenomena. In the case of TL, it has the form:

$$F_{TL-TUN}(t) = ln\left(1 + \frac{z\, s}{\beta}\, \int_{T_0}^{T} e^{-\frac{E}{k\,T}}\, dT\right). \tag{118}$$

For an LM-OSL peak, the function $F(t)$ takes the form:

$$F_{LMOSL-TUN}(t) = ln\left(1 + z\, \frac{\lambda\, t^2}{2P}\right). \tag{119}$$

Table 2
Symbols, Units and physical meaning of the parameters used in phenomenological models based on *localizedtransitions*.

a/a	Symbol	Units	Physical meaning
1	n_g	cm^{-3}	instantaneous concentrations of electrons (donors) in the ground state
2	n_e	cm^{-3}	instantaneous concentrations of electrons (donors) in the excited state
3	m	cm^{-3}	instantaneous concentration of holes (acceptors)
4	n	cm^{-3}	instantaneous concentration of all electrons (donors)
5	N	cm^{-3}	concentration of available electrons (donors) in TDDT
6	A	Function	Mathematical form of the stimulation mode
7	E	eV	Thermal activation energy
8	s	s^{-1}	Frequency factor
9	λ	$s-1$	optical stimulation wavelength
10	$\sigma(\lambda)$	cm^{-3}	optical absorption cross-section
11	ρ'	–	dimensionless number density of acceptors
12	τ_c	s^{-1}	critical tunneling lifetime
13	z		dimensionless constant equal to 1.8 introduced in the model.
14	B	s^{-1}	relaxation rate from the excited into the ground state

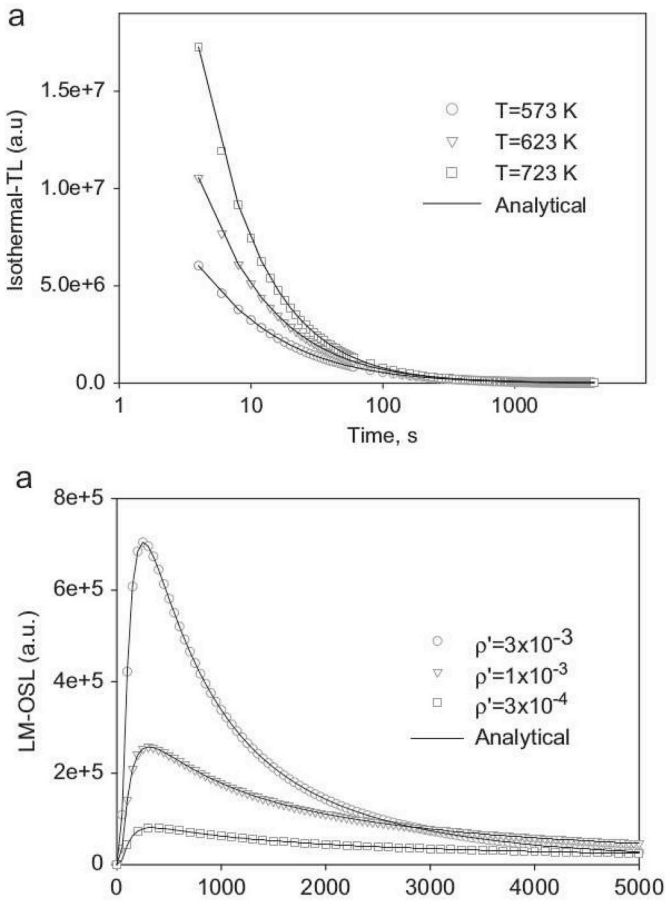

Fig. 10. (a) Comparison of the analytical Eqs. (116) and (120) with the solution of the system of Eq. (109) -(111), for the case of isothermal TL. (a) Three simulated isothermal TL signals are shown at temperatures T = 573, 623 and 733 K. (b) Comparison of the analytical Eqs. (116) and (119) with the solution of the system of Eq. (109) -(111), for the case of LM-OSL. Three simulated LM-OSL signals are shown for different values of the dimensionless parameter ρ' (Kitis and Pagonis, 2013).

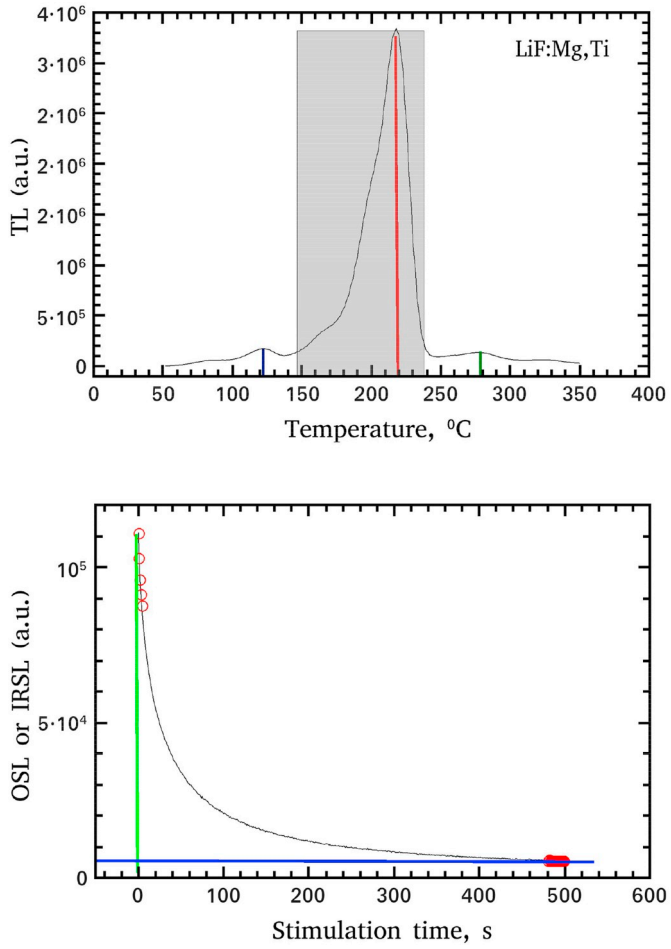

Fig. 11. (a) Analysis of TL signals: The intensity is measured either as "peak height" at the maximum temperature of a peak, or as the integrated area between two preselected temperatures. (b) Analysis of OSL or IRSL signals: The intensity is usually measured as the integrated signal of the first five channels, minus the mean value of the last twenty points of the curve.

For CW-OSL decay curves, the function $F(t)$ will be:

$$F_{CWOSL}(t) = ln(1 + z\,\lambda\,t). \quad (120)$$

Similar expressions to Eq. (120) apply for ITL and CW-IRSL signals, with the appropriate form of the constant λ.

The fifth master equation (Eq. (116)) was tested by comparing it with the numerical solution of the full system of differential equations in the tunneling model (Kitis and Pagonis, 2013, 2014; Pagonis and Kitis, 2015, Pagonis et al., 2013). Fig. 10 shows an example of such a comparison, showing very good agreement between the two approaches.

The fifth master equation has been also tested extensively during the past decade, by comparing it with many different types of experimental signals, from different types of natural and artificial dosimetric materials (Sfampa et al., 2014; Şahiner et al., 2014; Kitis et al., 2016a; b; Polymeris et al., 2017).

7. Analytical expressions in research and applications: analysis of complex experimental curves

In the preceding sections we presented the master analytical solutions of five specific phenomenological models. The analytical expressions are directly applicable to experimental data and allow the rapid and deep understanding of the properties of the system. The advantages of using the master equations are:

- The master equations retain all the properties and predictions of the system of differential equations from which they are derived.
- These equations hold for all stimulated luminescence modes commonly used in experiments.
- In order to use the master equations, the user needs to simply insert the appropriate stimulation function $p(t)$ for each experiment.

The analytical master expressions can be used to fit directly experimental data, whether they consist of a single component or of multiple components. The procedure to analyze a complex experimental curve into its individual components is called computerized curve deconvolution (CCD) analysis, and was originally developed for analysis of TL data (Bos et al., 1993, 1994; Horowitz and Yossian, 1995), and was generalized later to all SL phenomena. The application of CCD analysis to dosimeters leads to significant improvements in dosimetric techniques. For example, the dosimetric data in conventional TL readers are usually taken as the integrated area under a glow-curve (see Fig. 11), whereas in the case of hot gas readers the dosimetric data is used in the form of the total amount of light emitted during readout. For many dosimetric materials, extracting information from glow curves requires the application of complicated post-irradiation thermal or optical treatments, in order to erase the TL signal in the low temperature part of the dosimetric area (Horowitz, 1984). On the other hand, the TL signal in the temperature region above the dosimetric area cannot be used, and its removal is a very difficult task. These and other

practical problems are automatically removed by applying a CCD analysis to the experimental dosimetric glow curves.

An experimental glow curve analyzed by CCD is highly informative. For example in the case of TL, the information extracted from an experimental glow curve analyzed with the CCD consists of the following:

- The individual peaks in the glow-curve.
- The trapping parameters E and s of each peak, contributing thus to our basic understanding of the TL mechanism in the TL detectors.
- The exact integral of each glow-peak, which can be used to represent the dosimetric data,and to improve the accuracy of the dose evaluation.
- The background signal can be analyzed accurately, and the dosimetric TL signal can be determined even in the case of very low doses.

The successful application of CCD analysis is closely related to the concept of the superposition principle, which is discussed in some detail in section 12. In the next section we transform the five master equations, and bring them into a mathematical form which is easier to use for analyzing experimental data.

8. Bringing analytical expressions closer to experimental data: the transformed master equations

Early in the TL literature, researchers attempted to transform the original analytical equations by replacing the original variables, with equivalent parameters which can be directly evaluated from the experimental data. This idea of transforming the analytical equations was first achieved by Podgorsak et al. (1971) for a first order kinetics TL expression derived using a hyperbolic heating function. The next major step in this research area was taken by Kitis et al. (1998), who developed transformed equations for first, second and general order kinetics under a linear heating function. In later works transformed equations were developed by Kitis and Gomez Ros (1999); Gomez-Ros and Kitis (2002) for mixed order kinetics and for continuous trap distributions, and by Kitis et al. (2006a) for an exponential heating function. In the area of OSL, Kitis and Pagonis (2008) developed equations for LM-OSL signals. Recently Sadek et al. (2015a, b) transformed the analytical expression derived from the OTOR model, whereas Kitis and Pagonis (2014) developed transformed analytical expressions for tunneling recombination from the excited state of a trap.

We now describe the general method used for transforming the master equations in this paper. The description that follows is based on transforming analytical equations for TL, however it is very general and the exact same method can be applied to any of the master equations and experimental modes described in this paper.

The TL transformation is based on replacing two of the variables in the equations with two new variables, which can be estimated directly from the experimental data. Specifically the initial concentration of trapped electrons n_0 in the equations will be replaced with the maximum intensity I_m of the TL signal. In addition, the frequency factor s will be replaced with the temperature T_m at which the maximum TL signal occurs. Symbolically:

- $n_0 \rightarrow I_m$,
- $s \rightarrow T_m$.

In the case of LM-OSL signals, the optical excitation constant λ will be replaced with the time t_m at which the maximum LM-OSL signal occurs. Symbolically:

- $n_0 \rightarrow I_m$,
- $\lambda \rightarrow t_m$.

The transformation is based on the mathematical condition for the maximum of a peak-shaped TL or LM-OSL signals. The equations for the maximum signal intensity are among the most useful analytical expressions, in both theoretical and experimental research. These expressions are derived by equating the derivative of the stimulated luminescence intensity to zero, i.e. $dI/dt = 0$.

The algebra needed to transformed an analytical equation of the TL intensity from $I(n_o, E, s, b, T)$ into $I(I_m, E, T_m, b, T)$ is described in detail by Kitis et al. (1998) as follows:

Step 1: Consider, for example, the analytical GOK equation in its original form $I(n_o, E, s, b, T)$.
Step 2: Write this equation in the form $I_m(n_o, E, s, b, T_m)$, by replacing $T = T_m$.
Step 3: Divide the Equations in steps 1 and 2, to obtain the ratio I/I_m. In this step all parameters in front of the equation (like s, n_o etc) are eliminated. However, they are not eliminated from the main body of the equation.
Step 4: Use the condition for the maximum $dI/dt = 0$ to solve for the frequency factor s, and replace it in the main body of the equation. In this way the parameters s, n_o and the heating rate are eliminated. The algebra for this step may be extensive, but is always simple and straightforward.
Step 5: The resulting new equation will be the desired transformed master equation, $I_m(n_o, E, s, b, T_m)$.

It is noted that the above procedure is an exact transformation, and not an approximation of the original master equation. In the subsections that follow we present the transformed master equations, obtained using the above 5-step mathematical procedure.

8.1. Transforming the first master equation

8.1.1. Condition of maximum intensity for TL signals in the GOT/OTOR model

Sadek et al. (2015a) have transformed the first master equation obtained in section 3.4, from an expression of the form $I(n_0, E, s, R, T)$, into the form $I(I_m, E, T_m, R, T)$.

The condition for the maximum can be obtained by setting the derivative of Eq. (37) equal to zero, for both TL and LM-OSL. The final expression for the condition of the maximum of the TL peak in the OTOR/GOT model is:

$$\frac{\beta E}{k T_m^2} = F_{TL} s \exp\left[-\frac{E}{k T_m}\right], \tag{121}$$

with F_{TL} given by:

$$F_{TL} = \left[\frac{1}{1-R}\frac{1+2W\left[e^{z(T_m)}\right]}{\left(1+W\left[e^{z(T_m)}\right]\right)^2}\right]. \tag{122}$$

It is interesting to note here that Eq. (121) holds exactly for both the first and the second real branch of Lambert W function. We now consider separately the two cases studied previously, for values of the retrapping ratio $R > 1$ and $R < 1$.

8.1.2. Transformed first master equation for TL: case $c > 0$ $R < 1$

By following steps 1–3 outlined in section 8, we find:

$$I = I_m \exp\left(\frac{E(T-T_m)}{k\ T\ T_m}\right)\frac{W\left[e^{z_{1m}}\right] + W\left[e^{z_{1m}}\right]^2}{W\left[e^{z_1}\right] + W\left[e^{z_1}\right]^2}, \tag{123}$$

where z_1 is given by Eq. (38), and $z_{1m} = z_1$ at $T = T_m$.

In steps 4–5 of the procedure, the variables n_0, N, s are eliminated from the functions z_1 and z_{1m}, by using the condition for the maximum described by Eqs. (121) and (122). The result is:

$$z_1 = \frac{1}{c} - ln(c) + \frac{E\ e^{\frac{E}{k\ T_m}}}{k\ T_m^2}\frac{F(T,E)}{(1-R)\,F_{TL1}}, \tag{124}$$

where F_{TL1} is given by Eq. (122), and $F(T, E)$ is the exponential integral discussed in section 9.

Due to the complicated nature of F_{TL1}, it is useful to find a relation between F_{TL1} and the retrapping ratio R. For this reason, Sadek et al. (2015a) performed a simulation within a broad range of activation energies $(0.1 \le E \le 2.0)\, eV$ and frequency factors $(10^7 \le s \le 10^{19})\, s^{-1}$, which can be considered physically realistic (Chen, 1969a; b; Chen and Winer, 1970). From the simulation it was found that the following relations hold:

$$F_{TL1} = \frac{(1 - 1.05\, R^{1.26})}{(1 - R)}, \tag{125}$$

so that Eq. (124) becomes

$$z_1 = \frac{1}{c} - ln(c) + \frac{E\, e^{\frac{E}{k\, T_m}}}{k\, T_m^2} \frac{F(T, E)}{1 - 1.05\, R^{1.26}}. \tag{126}$$

Now, Eq. (123) along with Eqs (124) and (126) is the completely transformed first master equation, which can be used directly with experimental glow curves, when $R < 1$.

Summarizing, the transformed first master equation for $R < 1$ is:

Transformed first master equation for TL (GOT model, $R < 1$)

$$I = I_m\, e^{\left(\frac{E(T-T_m)}{k\, T\, T_m}\right)} \frac{W\left[e^{z_1 m}\right] + W\left[e^{z_1 m}\right]^2}{W\left[e^{z_1}\right] + W\left[e^{z_1}\right]^2}. \tag{127}$$

$$z_1 = \frac{1}{c} - ln(c) + \frac{E\, e^{\frac{E}{k\, T_m}}}{k\, T_m^2} \frac{F(T, E)}{1 - 1.05\, R^{1.26}}. \tag{128}$$

8.1.2. Transformed first master equation for TL: case $c < 0$ or $R > 1$

Working in the same manner as in the previous case when$R < 1$, we find for the OTOR analytical Eq. (49):

$$I = I_m\, e^{\left(\frac{E(T-T_m)}{k\, T\, T_m}\right)} \frac{W\left[-1, -e^{-z_{2m}}\right] + W\left[-1, -e^{-z_{2m}}\right]^2}{W\left[-1, -e^{-z_2}\right] + W\left[-1, -e^{z_2}\right]^2}, \tag{129}$$

where z_2 i s given by Eq. (44), and $z_{2m} = z_2$ the value at $T = T_m$. By eliminating n_0, N, s we find:

$$z_2 = \frac{1}{|c|} - ln(|c|) + \frac{E\, e^{\frac{E}{k\, T_m}}}{k\, T_m^2} \frac{F(T, E)}{(1 - R)\, F_{TL2}}. \tag{130}$$

The following relation between F_{TL2} and the retrapping ratio R was found by simulation:

$$F_{TL2} = \frac{(2.963 - 3.24\, R^{-0.74})}{|1 - R|}, \tag{131}$$

and Eq. (124) becomes:

$$z_2 = \frac{1}{|c|} - ln(|c|) + \frac{E\, e^{\frac{E}{k\, T_m}}}{k\, T_m^2} \frac{F(T, E)}{(2.963 - 3.24\, R^{-0.74})}. \tag{132}$$

Therefore, Eq. (129) along with Eqs. (130) and (132), is a completely transformed equation which is ready to use with experimental glow curves when $R > 1$.

In summary, when $R > 1$:

Transformed first master equation for TL (GOT model, $R > 1$)

$$I = I_m\, e^{\left(\frac{E(T-T_m)}{k\, T\, T_m}\right)} \frac{W\left[-1, -e^{-z_{2m}}\right] + W\left[-1, -e^{-z_{2m}}\right]^2}{W\left[-1, -e^{-z_2}\right] + W\left[-1, -e^{z_2}\right]^2}. \tag{133}$$

$$z_2 = \frac{1}{|c|} - ln(|c|) + \frac{E\, e^{\frac{E}{k\, T_m}}}{k\, T_m^2} \frac{F(T, E)}{(2.963 - 3.24\, R^{-0.74})}. \tag{134}$$

8.1.3. Condition of maximum intensity of LM-OSL signals in the GOT/OTOR model

By working in a similar manner, the following condition for the maximum is obtained for the case of LM-OSL signals:

$$t_m^2 = F_{LM-OSL} \frac{P}{\lambda}, \tag{135}$$

where

$$F_{LM-OSL} = \left[(1 - R) \frac{(1 + W\left[e^{z(t_m)}\right])^2}{1 + 2W\left[e^{z(t_m)}\right]}\right], \tag{136}$$

and t_m is the time corresponding to the maximum intensity I_m of the LM-OSL peak, and $W\left[e^{z(t_m)}\right]$ is the value of $W\left[e^{z(t)}\right]$ at $t = t_m$.

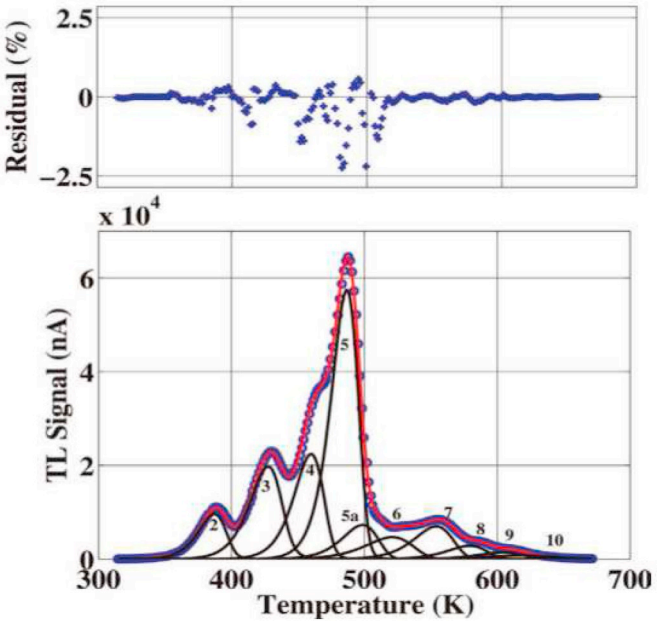

Fig. 12. The deconvolution of the RefGlow.009 glow-curve of the GLOCANIN project (Bos et al., 1994) using the transformed first master equations (Sadek et al., 2015a).

8.1.4. Using the first master equation to fit experimental data

Peng et al. (2016) implemented the transformed first master equation for $R < 1$, by developing a package within the open access software *R* (R Core Team, 2014). They also provided several examples of using this transformed equation with experimental data from different dosimetric materials.

Figs. 12 and 13 show examples of composite TL glow curves which were analyzed using the transformed first master equation, for two widely used dosimetric materials (Sadek et al., 2015a; Şahiner, 2017) (see Fig. 14).

Sadek et al. (2014b) have also developed transformed equations for experiments in which an exponential heating function is used. Fig. 4 shows an example of applying these additional transformed equations to fit experimental data for LiF:Mg,Ti (MTS).

8.2. Transforming the second master equation

8.2.1. Condition of maximum intensity for TL and LM-OSL signals in the MOK model

The mixed order kinetics is represented by Eq. (72). Let us apply the transformation method of section 8. In the case of TL signals described by the MOK model, the condition $dI/dT = 0$ gives the following general expression:

$$\frac{\beta\, E}{k\, T_m^2} = f\, s\, e^{-\frac{E}{k\, T_m}}, \tag{137}$$

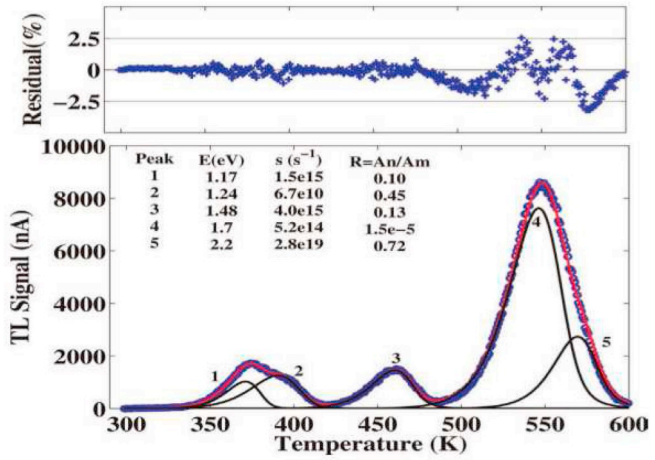

Fig. 13. The deconvolution of the natural CaF_2 glow-curve using the developed TL expressions. The FOM is 0.20% (Balian and Eddy, 1977). (Fig. 4, in Sadek et al. (2015).

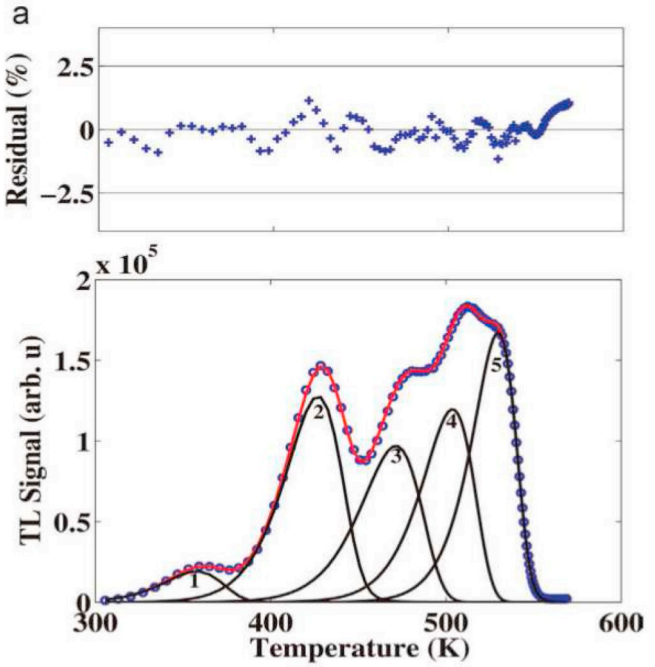

Fig. 14. Example of using the transformed first master equation, to fit experimental data obtained with an exponential heating function. The LiF:Mg,Ti (MTS, TLD-Poland) glow-curve was obtained using a hot nitrogen TL reader TL (15 s at 573 K), without post irradiation annealing. (Fig. 6 in Sadek et al. (2015).

where the factor f is:

$$f_{MOK-TL} = N_d\, g\, \frac{F_m + \alpha}{F_m - \alpha}, \tag{138}$$

and F_m is the value of the function $F(T)$ in Eq. (73) at $T = T_m$.

In the case of LM-OSL signals, condition dI/dt=0 for MOK gives:

$$t_m^2 = \frac{1}{\lambda} \cdot \frac{1}{g\, N_d} \cdot \frac{F_m - \alpha}{F_m + \alpha}, \tag{139}$$

where F_m is the value of $F(T)$ in Eq. (74) at $T = T_m$.

8.2.2. Transformed second master equation for TL (MOK model)

By following the same method as in section 8, we obtain:

$$I(T) = I(T_m)\, exp\left(\frac{E\,(T - T_m)}{k\; T\; T_m}\right) \frac{(F(T_m) - \alpha)^2}{F(T_m)}\, \frac{F(T)}{(F(T) - \alpha)^2}. \tag{140}$$

The function $F(T)$ is given by Eq. (73). Taking, now, into account the condition for the maximum given by Eq. (137) and Eq. (138), Eq. (73) becomes:

$$F(T) = exp\left(\frac{1}{f_{MOK}}\, \frac{T^2}{T_m^2}\, exp\left(\frac{E\,(T - T_m)}{k\; T\; T_m}\right)\left(1 - \frac{2\,k\; T}{E}\right)\right). \tag{141}$$

From this we obtain the value of $F(T_m)$ by setting $T = T_m$:

$$F(T_m) = exp\left(\frac{1 - (2\,k\; T_m)/E}{f_{MOK}}\right), \tag{142}$$

where the quantity f_{MOK} is given by Kitis and Gomez Ros (1999):

$$f_{MOK} = \frac{2.6 - 0.9203\,\alpha + 0.324\,\alpha^{3.338}}{2.6 - 2.9203\,\alpha + 0.324\,\alpha^{3.338}}. \tag{143}$$

In summary, the transformed second master equation for TL in the MOK model is:

Transformed second master equation for TL (MOK)

$$I(T) = I(T_m)\, exp\left(\frac{E\,(T - T_m)}{k\; T\; T_m}\right) \frac{(F(T_m) - \alpha)^2}{F(T_m)},\; \frac{F(T)}{(F(T) - \alpha)^2}$$

$$F(T) = exp\left(\frac{1}{f_{MOK}}\, \frac{T^2}{T_m^2}\, exp\left(\frac{E\,(T - T_m)}{k\; T\; T_m}\right)\left(1 - \frac{2\,k\; T}{E}\right)\right),$$

$$f_{MOK} = \frac{2.6 - 0.9203\,\alpha + 0.324\,\alpha^{3.338}}{2.6 - 2.9203\,\alpha + 0.324\,\alpha^{3.338}}.$$

8.2.3. Transformed second master equation for LM-OSL (MOK model)

For the case of LM-OSL signals described by the MOK model, we arrive to an equation similar to Eq. (141), but with different $F(t)$ and $F(t_m)$:

$$I(t) = I(t_m)\, \frac{t}{t_m}\, \frac{(F(t_m) - \alpha)^2}{F(t_m)}\, \frac{F(t)}{(F(t) - \alpha)^2}. \tag{144}$$

For the case of LM-OSL $F(t)$ is given by Eq. (74), which taking into account the condition for the maximum Eq. (139) becomes:

$$F(t) = exp\left(\frac{1}{2}\, \frac{t^2}{t_m^2}\, \frac{F(t_m) - \alpha}{F(t_m) + \alpha}\right), \tag{145}$$

and $F(t = t_m)$ is given by:

$$F(t_m) = exp\left(\frac{1}{2}\, \frac{F(t_m) - \alpha}{F(t_m) + \alpha}\right). \tag{146}$$

Eq. (144) cannot be used easily in its present form, but it can be brought into a more useful form as follows. A relation between $F(t_m)$ and α is found by a numerical simulation, and this relation is used to replace the term $F(t_m)$ with a function of α, so that Eq. (144) will be transformed into a three - parameter function, i.e. $I(I_m, t_m, \alpha, t)$. Such a relation between $F(t_m)$ and α is given by Kitis et al. (2009).

$$F(t_m) = 1.\,6476 - 1.0012\,\alpha + 0.357\,\alpha^2. \tag{147}$$

In summary, the transformed second master equation for LM-OSL signals in the MOK model is:

Transformed second master equation for LM-OSL (MOK)

$$I(t) = I(t_m)\, \frac{t}{t_m}\, \frac{(F(t_m) - \alpha)^2}{F(t_m)}\, \frac{F(t)}{(F(t) - \alpha)^2},$$

$$F(t) = exp\left(\frac{1}{2}\, \frac{t^2}{t_m^2}\, \frac{F(t_m) - \alpha}{F(t_m) + \alpha}\right),$$

$$F(t_m) = 1.\,6476 - 1.0012\,\alpha + 0.357\,\alpha^2.$$

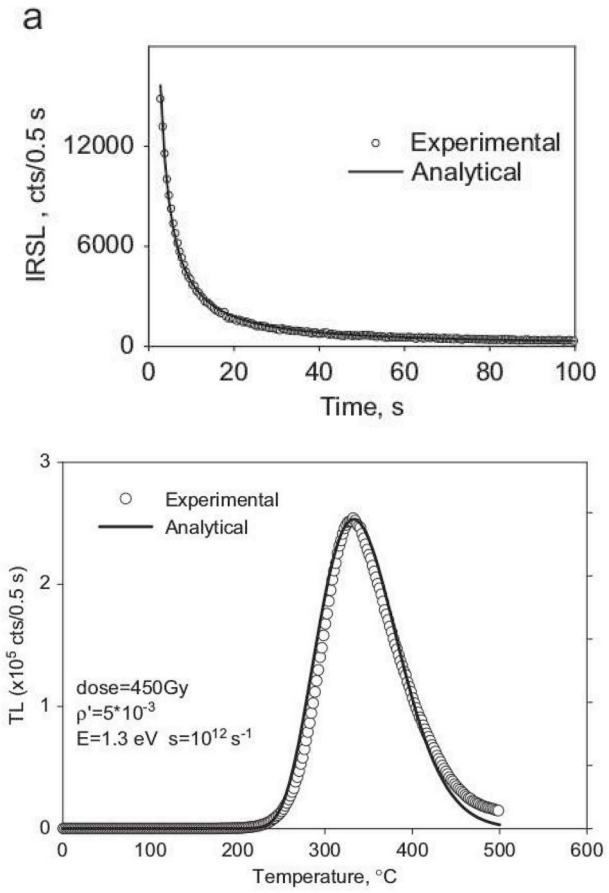

Fig. 15. Fitted experimental data from Kitis and Pagonis (2013).

8.3. Transforming the third, fourth and fifth master equations

It is noted that the transformed version of the third and fourth master equations have not been developed yet in the literature. It is expected that the transformed equations for the fourth master equation (NMTS model) will be similar to those for the GOT model, but not identical, due to the mathematical differences between these two models.

It is also noted that Kitis and Pagonis (2014) developed the transformed fifth master equation. The result of the transformation is rather complex, with the details given in their paper. In practical work, we have found it easier to fit experimental data by using the fifth master equation in its original form, and several examples of fitted data are given in the next subsection.

8.3.1. Using the fifth master equation to fit experimental data

Fig. 15 shows experimental TL, LM-OSL and LM-IRSL data which were fitted using the original analytical equations by Kitis and Pagonis (2013). During the last decade there have been many applications of the fifth master equation in describing tunneling effects in a variety of dosimetric materials (Kitis et al., 2006a; b; Pagonis et al., 2017; Polymeris et al., 2017; Şahiner et al., 2014; Sfampa et al., 2014).

9. The exponential integral in the master equations

Most of the master equations in this paper contain the exponential integral $\int_{T_0}^{T} e^{-\frac{E}{kT'}}\,dT'$. Basically there are two numerical methods to evaluate this important quantity: (a) As a elementary function in available software and (b) Through approximate analytical expressions. In this section we present these two methods.

9.1. Elementary function methods

The exponential integral function $Ei[z]$ has been implemented as an elementary built-in function similar to sine, cosine etc, in almost all existing software. The exponential integral can be evaluated as a function of the $Ei[z]$ function.

When the thermal stimulation takes place through a linear heating function, we use the expression:

$$\int_{T_0}^{T} e^{-\frac{E}{kT'}}\,dT' = T\,exp\left(-\frac{E}{kT}\right) + \frac{E}{k}Ei\left[-\frac{E}{kT}\right]\Big|_{T_0}^{T}. \tag{148}$$

When the thermal stimulation takes place through a exponential heating function, we use:

$$\int_{T_0}^{T} \frac{e^{-\frac{E}{kT'}}}{T_g - T'}dT' = -exp\left(-\frac{E}{kT_g}\right)Ei\left[\frac{E}{kT_g} - \frac{E}{kT}\right] + Ei\left[-\frac{E}{kT}\right]\Big|_{T_0}^{T}, \tag{149}$$

where T_g is the hot gas temperature (see below).

9.2. Approximation method

In cases where the exponential integral function $Ei[z]$ is not implemented as a built-in function, one has to use its analytical approximations. There are two appropriate approximations, depending upon the value of its argument z. When $z = E/k\,T > 14$, the appropriate approximation is the asymptotic series approximation (ASA) (Chen, 1971, 1974; Chen and McKeever, 1997; Kitis et al., 2006a,b):

$$-Ei(-z) = e^{-z}\sum_{n=0}^{N}\frac{(-1)^n n!}{z^{n+1}}. \tag{150}$$

In practice, three terms of the ASA in Eq. (150) give very satisfactory results.

On the other hand when $z = E/k\,T < 14$, the appropriate approximation is the convergent series approximation (CSA) given by Chen and McKeever (1997); Kitis et al., 2006a):

$$Ei(-z) = \gamma + ln(z) + \sum_{n=1}^{\infty}\frac{(-z)^n}{n\cdot n!}, \tag{151}$$

where $\gamma = 0.5772156649$ is the Euler constant.

In the case of CSA there is a question about the number of terms needed for an accurate approximation in the whole region of $|z|$ between 14 and 0. It is found that using 50 terms of the CSA, the exponential integral is very accurately approximated up to $|z| = 14$, as is shown in Fig. 16b. Curve (a) of Fig. 16 shows the ASA approximation with $N = 10$. For z greater than 10, the ASA approximation must be used with the accuracy being kept at the sixth significant figure, by increasing appropriately the number of terms in Eq. (150). For $|z|$ between 14 and 0, the ASA must be used with the accuracy being kept at the sixth significant figure, by decreasing the number of terms in Eq. (151).

10. Bridging the gap between 1^{st} and 2^{nd} order kinetics

10.1. The empirical general order kinetics (GOK)

In a previous section we showed that under specific physical assumptions, the OTOR model leads to TL peaks characterized by first and second order kinetics. We can then consider first and second order kinetics as two boundary conditions of the OTOR physical model. However, experimentalists have reported many cases where the shape of the TL glow curves deviates from first and second order kinetics. Such deviations from first and second order can be described within the framework of the OTOR model, by considering A_n values larger than A_m ($A_n \geq A_m$). In order to describe this kind of TL peaks, Halperin and Braner (1960) proposed the usage of the geometrical characteristics of TL peaks, shown schematically in Fig. 17.

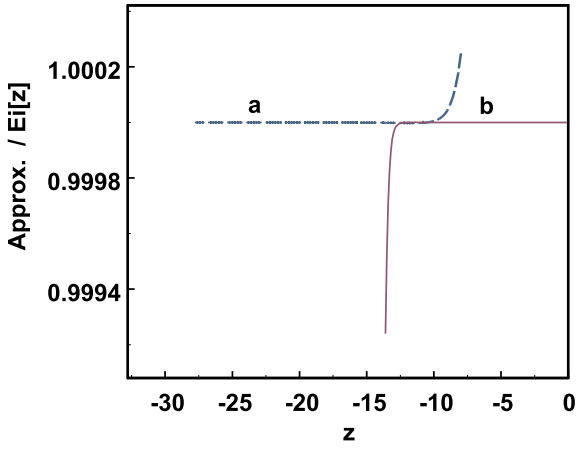

Fig. 16. Approximation to the exponential integral. (a) For the asymptotic series approximation (ASA) method of evaluating the exponential integral, taking 10 terms plus one half of the $11-th$ is recommended. A somewhat better approximation can be reached by taking all the terms down to the smallest one in absolute value and adding one half of the next one and (b) Convergence series approximation (CSA) method of evaluating the exponential integral taking into account 50 terms. From Kitis et al. (2006a).

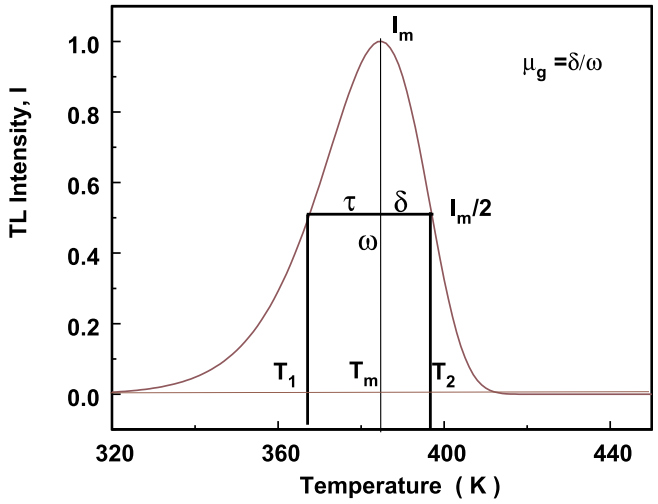

Fig. 17. Definitions of the geometrical characteristics of a single TL peak.

The geometrical characteristics of a single glow–peak shown in Fig. 17 are the peak maximum temperature T_m, and the temperatures T_1 , T_2 at half maximum TL intensity on the low and high temperature side of the glow peak respectively. These quantities are used to define further the widths $\omega = T_1 - T_2$, $\delta = T_2 - T_m$ and $\tau = T_m - T_1$. Additionally, one can characterize the shape of the glow peak by using two area parameters n_0 and n_m, representing the total integral and the high temperature half integral of the glow peak respectively. Based on the above parameters, Halperin and Braner (1960) suggested that the symmetry of each peak can serve as an indicator of the kinetic order, and defined the following two symmetry factors:

$$\textit{Geometrical symmetry factor}: \quad \mu_g = \frac{\delta}{\omega}. \tag{152}$$

$$\textit{Integral symmetry factor}: \quad \mu_g{}' = \frac{n_m}{n_0}. \tag{153}$$

The geometrical symmetry factor μ_g is clearly geometrical, and can be obtained directly from experimental data. Its value is $\mu_g = 0.42$ for first order kinetics and $\mu_g = 0.52$ for second order kinetics. The integral symmetry factor $\mu_g{}'$ has values which are very close to those of the geometrical symmetry factor μ_g. Kitis and Pagonis (2007) and Kitis et al. (2008), showed that $\mu_g{}'$ also has a clear functional relationship with the kinetic parameters of the model.

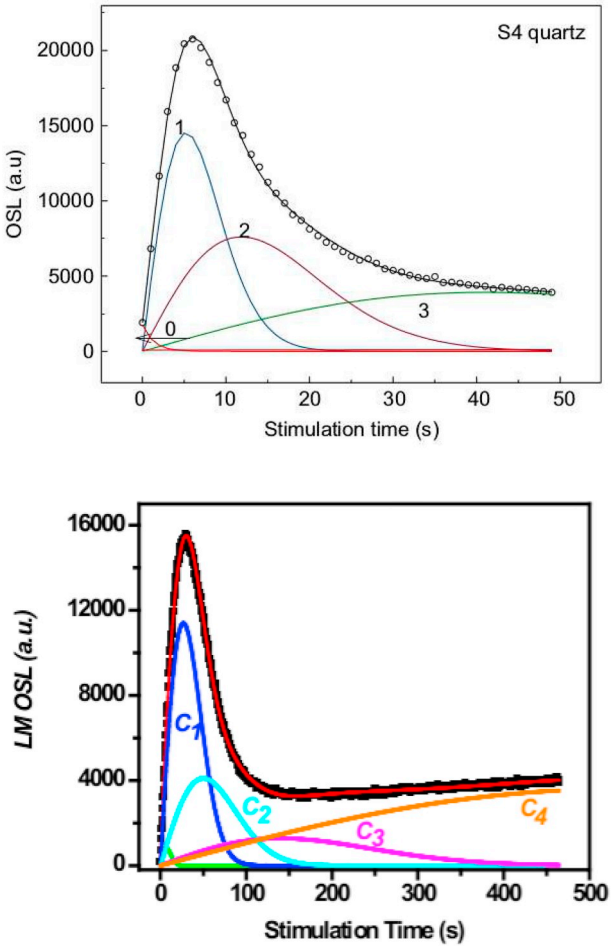

Fig. 18. Examples of CCD of LM-OSL curves for quartz samples, after Oniya et al. (2012) and Kitis et al. (2011).

In view of the experimentally reported shapes of TL glow peaks with symmetry factors $0.42 < \mu_g < 0.52$, there is clearly a need to account for such intermediate kinetic orders $1 < b \leq 2$. This gap between first and second order kinetics was investigated by the introduction of mixed order kinetics by Chen et al. (1981) and also by the introduction of the empirical general order kinetics model by May and Partridge (1964). In the next subsection we will present the empirical GOK model, and in section 10.8 we discuss the relationship between the GOK, MOK and OTOR models.

10.2. The GOK equation for TL

The GOK model, although empirical, has been widely accepted by the research community and has become one of the cornerstones of both theoretical and experimental research in TL and OSL.

The differential equation for TL in the GOK model is (May and Partridge, 1964; Rasheedy, 1993; Chen and Kirsh, 1981; Chen and McKeever, 1997):

$$I_{TL} = -\frac{dn}{dt} = \frac{n^b}{N^{b-1}} s\, e^{-\frac{E}{kT}}. \tag{154}$$

The quantity b is the kinetic order, which takes values $1 < b \leqq 2$.

10.3. GOK solutions for TL measured with a linear heating function

Most TL experiments involve a linear heating function of the form:

$$T = T_0 + \beta\, t, \tag{155}$$

where T_0 the starting temperature. Assuming this constant heating rate β, the solution of Eq. (154) is:

$$I_{TL}(T) = n_0 \left(\frac{n_0}{N}\right)^{b-1} \frac{s}{\beta}\, e^{-\frac{E}{k\,T}} \left[1 + (b-1)\left(\frac{n_0}{N}\right)^{b-1} \frac{s}{\beta} \int_{T_0}^{T} e^{-\frac{E}{k\,T'}} dT'\right]^{-\frac{b}{b-1}}. \tag{156}$$

The dimensions of $I_{TL}(T)$ can be shown once more to be $cm^{-3}\,K^{-1}$, in agreement with the units encountered for the luminescence intensity in the OTOR, MOK and NMTS models.

The general order kinetics expression of Eq. (156), although empirical, it was proved to be an extremely successful and useful equation. For $b = 2$ it is identical with the second order kinetics Eq. (25). On the other hand, for b values infinitesimally higher than 1, e.g. $b = 1.001$, Eq. (156) approaches the first order kinetics Eq. (22) to any desired accuracy. Obviously this makes the separate use of first and second order kinetic equations as curve fitting functions unnecessary, since the same Eq. (156) can be used for any value of the kinetic order b.

10.4. GOK solutions for TL measured using an exponential heating function

Another heating function widely used in commercial TLD readers is the exponential heating function, first proposed by Osada (1960) and used in TL analysis by Gomez Ros et al. (1993), Dijk van and Julius (1993); Dijk van and Busscher (2002), for the case of stable temperature hot gas TL readers in the form:

$$T(t) = T_g - (T_g - T_0)e^{-\alpha t}, \tag{157}$$

where T_g is the hot gas temperature which the gas reader approaches asymptotically with time, and T_0 is the temperature at $t = 0$, with α given by the expression:

$$\alpha = \frac{\delta\, A}{m\, c_p}, \tag{158}$$

where δ is the heat transfer efficiency, A is the heated area, m the mass of the sample and c_p the heat capacity.

This hot gas TL reader heating scheme is the one we get "naturally", if we let a cold sample warm up to the environment, while being in thermal contact with an infinite thermal bath at temperature T_g. This situation exists in the stable temperature hot gas TL readers, where the "cold" TL chip is initially at room temperature, and is then inserted in the readout chamber, which is at the much higher temperature T_g of the hot gas.

Working in a similar manner as for linear heating, the general order equation for exponential heating is (Kitis et al., 2006a):

$$I(T) = n_0 \left(\frac{n_0}{N}\right)^{b-1} \frac{s}{\beta}\, e^{-\frac{E}{kT}} \left[1 + (b-1)\left(\frac{n_0}{N}\right)^{b-1} \frac{s}{\beta} \int_{T_0}^{T} \frac{e^{-\frac{E}{kT'}}}{T_g - T'} dT'\right]^{-\frac{b}{b-1}}. \tag{159}$$

The dimensions for $I(T)$ in this equation are similar to those of Eq. (156).

10.5. GOK solutions for linearly modulated -OSL

The concept of general order kinetics was introduced by Bulur (1996) and Bulur and Goksu (1999), who formulated the GOK model for OSL, and especially for the description of linearly modulated OSL signals (LM-OSL).

In LM-OSL experiments the intensity of the optical excitation source is linearly increased with time, and the general order kinetic equation becomes:

$$\frac{dn}{dt} = -\frac{\lambda_{LM-OSL}}{P} \frac{n^b}{N^{b-1}}\, t, \tag{160}$$

where

$$\lambda_{LM-OSL} = \alpha\, I, \tag{161}$$

and α (cm^2) is the optical stimulation cross section, I ($photons\ cm^{-2}\ s^{-1}$) is the illumination photon flux and P the total illumination time.

The solution of Eq. (160) gives:

$$I(t) = N_0\, \alpha\, I\, \frac{t}{P} \left[1 + (b-1)\, \frac{\lambda\, t^2}{2\, P}\right]^{-\frac{b}{b-1}}, \tag{162}$$

where N_o is the initial concentration of trapped electrons

10.6. GOK solutions for CW-OSL and prompt isothermal decay of TL

When the stimulation is performed using a constant illumination intensity or constant temperature, we have the case of continuous wave OSL (CW-OSL) or prompt isothermal decay experiments (PID or ITL). According to Bulur (1996) the differential equation in this case is:

$$\frac{dn}{dt} = -\lambda\, \frac{n^b}{N^{b-1}}. \tag{163}$$

Eq. (163) can describe these two different luminescence phenomena, with the following decay constants:

$$\lambda_{OSL} = \alpha\, I_0, \tag{164}$$

$$\lambda_{ITL} = s\, exp\left(-\frac{E}{k\, T_{dec}}\right). \tag{165}$$

The decay constant λ_{OSL} of Eq. (164) corresponds to CW-OSL processes, whereas the decay constant λ_{ITL} of Eq. (165) corresponds to an isothermal decay of TL at a constant temperature T_{dec}.

The solution of Eq. (163) gives

$$I(t) = I_0\, [1 + (b-1)\lambda\, t]^{-\frac{b}{b-1}}, \tag{166}$$

with $I_0 = n_0\lambda$, and n_0 is the initial concentration of trapped electrons.

Eq. (166) means that CW-OSL and ITL signals are described by the same mathematical formula. During ITL the sample is held at a preselected constant temperature, and remains at this temperature for time t emitting light; this process is called prompt isothermal decay (PID). After the end of the PID, the sample is heated from room temperature to $500 - 600^oC$, in order to obtain the residual TL glow curve (R-TL). The behavior of the R-TL as a function of both decay temperature and decay time, is called residual isothermal decay (RID).

10.7. Transformed equations for the GOK model

In this section we present the transformed equations in the GOK model, for both TL and LM-OSL peak-shaped signals.

10.7.1. Transformed TL equations for GOK: linear heating function

In the case of TL signals described by the GOK models, the condition $dI/dT = 0$ gives the following general expression:

$$\frac{\beta\, E}{k\, T_m^2} = f\, s\, e^{-\frac{E}{k\, T_m}}, \tag{167}$$

where the factor f is:

$$f_{GOK-TL} = \left(\frac{n_o}{N}\right)^{b-1} \left[1 + (b-1)\, \frac{2\, k\, T_m}{E}\right]. \tag{168}$$

By using these equations, Kitis et al. (1998) transformed the first, second and general order kinetics equations under a linear heating function, from the mathematical form $I(n_o, E, s, b, T)$ into the transformed equations $I(I_m, E, T_m, b, T)$.

There are two possible transformations of Eq. (156), depending on the way the exponential integral is evaluated (see section 9).

By considering the asymptotic series approximation described in

section 9, the transformed GOK Eq. (156) becomes:

$$I(T) = I_m\, b^{\frac{b}{b-1}}\, exp\left(\frac{E}{k\,T}\,\frac{T-T_m}{T_m}\right)\left[(b-1)\,(1-\Delta)\frac{T^2}{T_m^2}\,,\right.$$
$$\left. exp\left(\frac{E}{k\,T}\,\frac{T-T_m}{T_m}\right) + Z_m\right]^{-\frac{b}{b-1}} \tag{169}$$

with $\Delta = 2\,k\,T/E$, $\Delta_m = 2\,K\,T_m/E$ and $Z_m = 1 + (b-1)\Delta_m$

By considering the elementary function method, the transformed GOK 156 becomes:

$$I(T) = I_m\, e^{\left[-\frac{E}{k\,T}\cdot\frac{T_m-T}{T_m}\right]}\cdot\left[1 + \frac{b-1}{b}\,\frac{E}{k\,T_m^2}\,e^{\frac{E}{k\,T_m}}\{F(E,\,T) - F(E,\,T_m)\}\right]^{-\frac{b}{b-1}}, \tag{170}$$

where Eq. (148) becomes:

$$F(E,\,T) = \int_{T_0}^{T} e^{-\frac{E}{kT'}}\,dT' = T\,e^{-\frac{E}{k\,T}} + \frac{E}{k}\,Ei\left[-\frac{E}{k\,T}\right], \tag{171}$$

which for $T = T_m$ takes the form:

$$F(E,\,T_m) = \int_{T_0}^{T_m} e^{-\frac{E}{kT'}}\,dT' = T_m\,e^{-\frac{E}{k\,T_m}} - \frac{E}{k}\,Ei\left[-\frac{E}{k\,T_m}\right]. \tag{172}$$

10.7.2. Transformed TL equations for GOK: exponential heating function

Using again the general method presented in section 8, and considering the exponential integral function given from Eq. (174) in section 9, the transformed general order kinetics equation is (Kitis et al., 2006a):

$$I(T) = I_m\, exp\left(-\frac{E(T_m-T)}{kTT_m}\right)\times$$
$$\times\left(1 - \frac{(b-1)(T_g-T_m)E}{bkT_m^2}\,exp\left(\frac{E}{kT_m}\right)(F(T_m,\,T_g,\,E) - F(T,\,T_g,\,E))\right)^{-\frac{b}{b-1}}. \tag{173}$$

where

$$F(T,\,T_g,\,E) = -exp\left(-\frac{E}{kT_g}\right)Ei\left(\frac{E}{kT_g} - \frac{E}{kT}\right) + Ei\left(-\frac{E}{kT}\right). \tag{174}$$

10.7.3. Transformed LM-OSL equations for GOK

The transformation from $I(n_0, E, s, b, T) \rightarrow I(I_m, E, t_m, b, T)$ for general order kinetics can be applied to LM-OSL signals as well. The form of the transformed LM-OSL equation was given by Kitis and Pagonis (2008):

$$I(t) = I_m\,\frac{t}{t_m}\left[\frac{b-1}{2\,b}\,\frac{t^2}{t_m^2} + \frac{b+1}{2}\right]^{\frac{b}{1-b}}. \tag{175}$$

10.7.4. Using the GOK equations to fit experimental data

Figs. 19 and 20 show examples of applying the transformed GOK equations for TL and PID signals, in the dosimetric material Lithium tetraborate (LBO).

10.8. Discussion: the relationship between GOK, MOK and OTOR models

This subsection discusses the relationship between the first master equation obtained from the OTOR model, and the well known empirical general order kinetics equation for stimulated luminescence phenomena. The gap between first and second order kinetics phenomena can be bridged by using one of two approaches: by using *either* the analytical solutions of OTOR and NMTS based on the Lambert function, *or* by using the empirical general order kinetics and mixed order kinetics.

Fig. 21 shows the relationship between the retrapping rate (R) in the GOT/OTOR model, and the empirical kinetic order constant b. The curves in this graph are obtained for different values of the trap filling ratio N/n_o.

There have been several discussions about the use of GOK in the

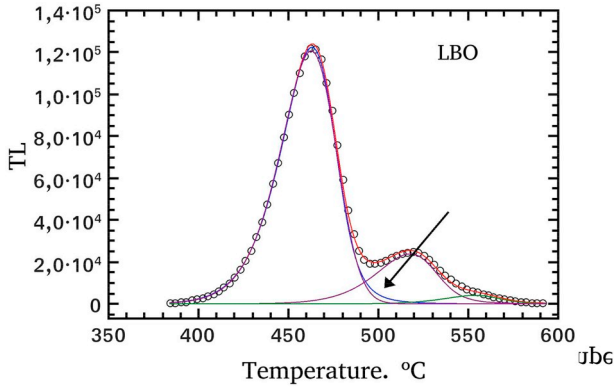

Fig. 19. CGCD analysis of TL glow-curve for LBO using general order kinetics and the first master equation. Both equations gave excellent fit. The differences between the two expressions are restricted at the high temperature end of the glow-peak, indicated by the arrows. From Kitis et al. (2016b).

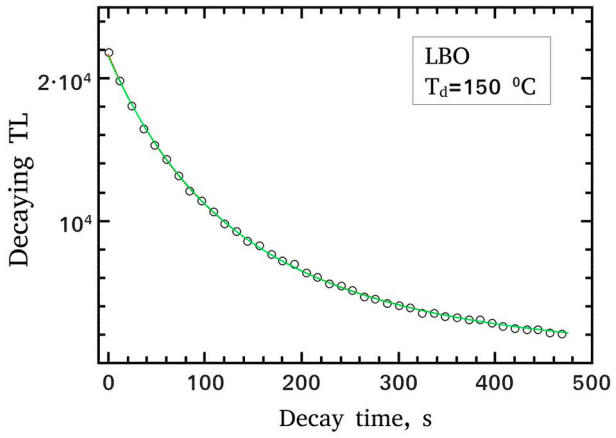

Fig. 20. An example of a PID curve for LBO, analyzed using the GOK and the first master equation. Both equations gave identical fits.

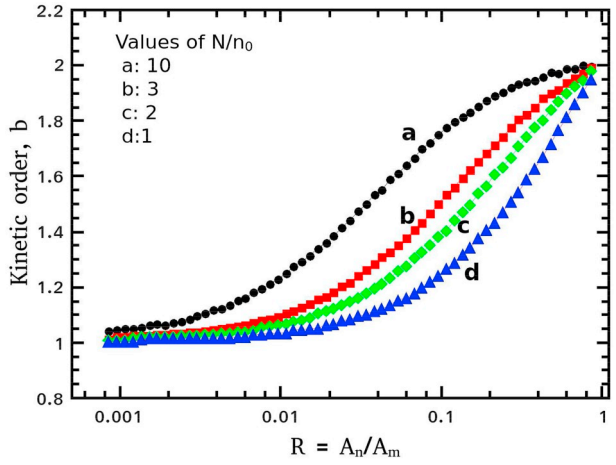

Fig. 21. The kinetic order parameter b characterizing the GOK model, as a function of he retrapping ratio $R = A_n/A_m$ in the GOT/OTOR model, for different values of the trap filling N/n_o. The A_n and A_m values were randomly selected from the interval of 10^{-10} to 10^{-7} cm^3s^{-1}, and the kinetic parameters were $E = 1$ eV and.$s = 10^{12}s^{-1}$.

literature (Piters and Bos, 1993; Sunta et al., 1999, 2001, 2002a, 2002b, 2005) and generally on the validity of the TL (Kelly et al., 1968; Kelly and Braunlich, 1970; Opanowicz, 1992; Lewandowski and McKeever, 1991), with some authors questioning the validity of both the Randall-Wilkins equation, and of the empirical general order kinetics equation.

The extensive work by Sadek et al. (2014) and Sadek and Kitis (2017) provided a detailed and extensive comparison between the GOK and the analytical solutions of the OTOR model. These authors tested the validity of using general order kinetics, by simulating the existing methods for determining the activation energy of a single glow peak. The simulations were carried out for a wide range of kinetics parameters, as follows:

- Step 1: A set of TL glow peaks was generated as numerical solutions of the differential Eqs. (5)–(7), by using a range of model parameters.
- Step 2: The activation energy E of the TL glow peaks was evaluated using the following peak shape equations proposed by Kitis and Pagonis (2007) for GOK, and by Kitis et al. (2008) for the MOK models:

$$GOK:\ E = C_\omega \cdot b^{\frac{b}{b-1}} \cdot \frac{k\,T_m^2}{\omega} - 2kT_m, \tag{176}$$

$$MOK:\ E = C_\omega \cdot \frac{k\,T_M^2}{\omega} \cdot \frac{1}{\mu'_g} \cdot \frac{1+\alpha(2\,\mu'_g-1)}{1+\alpha(\mu'_g-1)}, \tag{177}$$

$$C_\omega = \frac{\omega\, I_m}{\beta\, n_0}. \tag{178}$$

The kinetic order b and the mixed order parameter α were evaluated iteratively, by using the value of integral symmetry factor μ'_g:

$$GOK:\ \mu'_g = \left[\frac{b}{1+(b-1)\frac{2\,k\,T_m}{E}}\right]^{-\frac{1}{b-1}}, \tag{179}$$

$$MOK:\ \mu'_g = \frac{1-\alpha}{F_m-\alpha}, \tag{180}$$

$$F_m = 2.58226 - 3.13911\,\alpha + 0.55071\,\alpha^2.$$

- Step 3: The activation energy E of the TL glow peaks was also evaluated using the CGCD technique, based on the GOK expression Eq. (156).

The results of Sadek et al. (2014) in the above study are shown in Fig. 22. The activation energy values were calculated using the GOK peak shape method for 500 random glow peaks generated with a heating rate $\beta = 1$ K/s and for the range of $R = A_n/A_m$ from 10^{-3} to 10^3, with different trap occupancy concentrations n_0/N. The A_n and A_m values were randomly selected in the interval of 10^{-10} to $10^{-7}\ cm^3s^{-1}$. The input values of the kinetics parameters were $E = 1\ eV$ and $s = 10^{12}\ s^{-1}$. The trap occupancy concentration is denoted beside each curve in Fig. 22.

The agreement between input and output values of the activation energy was taken as the criterion for the success or failure of the GOK and MOK equations.

Fig. 22 consists of two distinct regions. In the first region defined by $A_n < A_m$ or $R < 1$, the accuracy of the GOK model is very good near the limits of first order kinetics ($A_n \lll A_m$), and second order kinetics ($A_n \approx A_m$). Between these two limits, the maximum deviation of the general order kinetics from the OTOR generated peaks is of the order of 4% at around $b = 1.7$. For experimental TL peaks, this 4% deviation becomes important only when the accuracy of experimental data is much better than 4%. Sadek et al. (2014) concluded that in experimental applications, the GOK equation works very well for $1 < b \leqq 2$.

In the second region in Fig. 22 defined by $A_n > A_m$ or $R > 1$, the

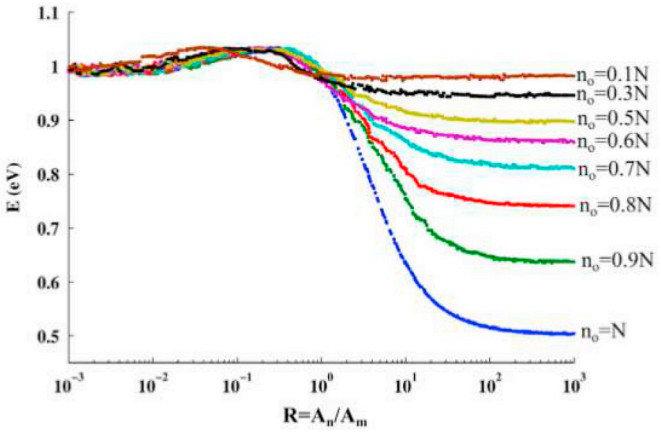

Fig. 22. The activation energy values calculated using the GOK peak shape method for 500 glow peaks generated with heating rate 1 K/s over a wide range of $R = A_n/A_m$ from 10^{-3} to 10^3 , with different trap occupancy concentrations (n_0/N). The kinetics parameters were E = 1 eV and s = 10^{12} s^{-1} The trap occupancy concentration is denoted beside each curve.

GOK model fails completely to describe the OTOR generated TL peaks for values of $n_0/N > 0.3$. In the luminescence literature, it is more or less accepted that the general order kinetics has no physical meaning for $b > 2$.

10.8.1. *Comparison of the first GOT master equation with the MOK, NMTS models*

In their extended study, Sadek et al. (2014) also have investigated the success and failure of the first master equation in this paper for the GOT model (Kitis and Vlachos, 2013). They applied the first master equation to 50 glow peaks generated by the OTOR model, using the same procedure described above. The glow peaks were evaluated for values of R from 10^{-3} to 10^3, and the A_n , A_m values were randomly selected from the interval of $10^{-10} - 10^{-7}\ cm^3s^{-1}$. The rest of the kinetic parameters were $n_0 = N = 10^{10} cm^{-3}$, $E = 1\ eV$ and s = 10^{12} s^{-1}The results are shown in Fig. 23, where the first master analytical expressions is seen to describe accurately the glow peaks generated by the OTOR model, over the full range of $R = A_n/A_m$. The error did not exceed 0.5% in all cases, whether $R < 1$ or $R > 1$. The activation energy values and the corresponding FOM (%) were calculated by the CGCD algorithm, and the E values were also calculated by using the analytical expressions deduced by Kitis and Vlachos (2013).

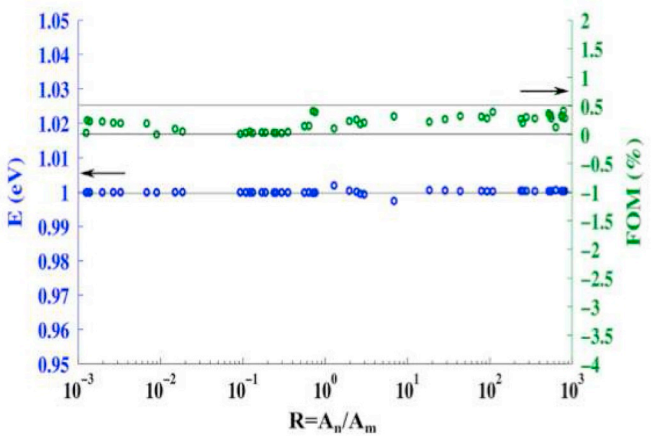

Fig. 23. The activation energy values calculated by the CGCD algorithm using the analytical expressions deduced by Kitis and Vlachos (2013), and the corresponding FOM (%) for 50 glow peaks generated with a heating rate 1 K/s, over a wide range of R from 10^{-3} to 10^3. The kinetic parameters were $n_0 = N = 10^{10} cm^{-3}$, E = 1 eV and s = 10^{12} $s.^{-1}$

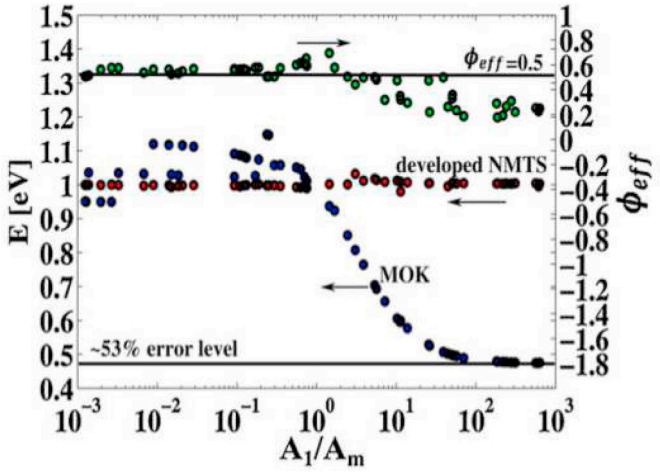

Fig. 24. E_{MOK}, E_{NMTS} and φ_{eff} obtained by the peak-fitting method, using the MOK and the master equations for the NMTS model, with different values of $R = A_1/A_m$. The kinetics parameters were: $X = 10^8\, cm^{-3}/s$, $N_1 = 10^{12}\, cm^{-3}$, $N_2 = 4 \times 10^{10} cm^{-3}$, $M_1 = 1.01 \times 10^{12} cm^{-3}$, $A_1 = 4 \times 10^{-9} cm^3/s$, $A_2 = 10^{-7} cm^3/s$, $B = 10^{-9} cm^3/s$, $A_m = 10^{-9} cm^3/s$, $E = 1\, eV$, $s = 4 \times 10^{12}\, s^{-1}$ and $\beta = 1K/s$.

Sadek et al. (2015b) also compared the second master analytical TL expression (MOK model), with the analytical TL expression for the NMTS model given by Eq. (84), (86) and Eqs. (88) and (90). Their results are shown in Fig. 24, where one can see that the MOK analytical TL expressions describe in a relatively satisfactory manner the TL peaks generated by the IMTS model for $R < 1$, but they fail completely for $R > 1$. On the other hand the NMTS analytical TL expressions given by Eqs. (84 and 86) and Eqs. (88 and 90) describe accurately the TL peaks generated by the IMTS model.

Sadek et al. (2015b) also performed extensive tests in the case of TL peaks generated by the IMTS model. The tests were based on the comparison between the input and output values of activation energy E, and on the goodness of fit expressed by the figure of merit (FOM) (Balian and Eddy, 1977). The analytical equations used by Sadek et al. (2015b) were the analytical GOK Eq. (156), the analytical MOK Eqs. (72) and (73), the analytical OTOR TL expressions (Eqs (37) and (49), and finally the general and mixed order peak shape methods (Kitis and Pagonis, 2007; Kitis et al., 2008), which have been described in detail in section 10.8.

In conclusion, the detailed study of Sadek et al. (2014) showed that the GOK and MOK analytical TL expressions are accurate in the region $R < 1$, but fail completely in the region $R > 1$ where the errors in the output E values can be of the order of 50% when $R \gg 1$. The GOK expression becomes accurate only for low doses, when $n_o/N < 0.3$. The master equations based on the NMTS model were derived using the Lambert $W(z)$ function, and can accurately describe the NMTS glow peaks, even in cases where the GOK and MOK analytical TL expressions failed.

The TL expressions based on the OTOR model using the Lambert-W function (Eqs (37), (49)) can be used to fit TL peaks generated by the IMTS and NMTS models even when $R \gg 1$.

11. Transforming shapeless signals into peak shaped curves

In the previous sections we presented the five master equations, and transformed several of them into equations suitable for fitting experimental data. The transformation method described in section 8 can derive families of analytical expressions which depend upon variables that can be extracted directly from experimental curves. Further examples, in addition to those presented in this article, are the transformation equations by Sadek et al. (2015) for analytical OTOR equation under an exponential heating function, and by Sadek et al. (2015b) for the analytical NMTS equation.

The stimulated luminescence signals in CW-OSL, ITL and CW-IRSL experiments do not provide peaked shape curves, but are featureless decay curves. For such featureless monotonic signals, the transformation method in section 8 can not be used, and one must use specialized methods to transform the featureless curves into peak shaped signals. These methods were presented in a unified presentation in the paper by (Chen and Pagonis, 2008) and are summarized also in the following subsections.

11.1. TL-like presentation

We will demonstrate this kind of transformation using the general order kinetics equation for isothermal processes, which according to Kirsh and Chen (1991) is:

$$I(t) = I_0\,[1 + (b-1)\lambda\, t]^{-\frac{b}{b-1}}, \tag{181}$$

with $I_0 = n_0/\tau$ and $\lambda = 1/\tau$ is the decay constant of the isothermal process. Following Kirsh and Chen (1991) and Chen and Pagonis (2008) let us define

$$x = ln(t), \tag{182}$$

or ($t = e^x$). By multiplying both sides of Eq. (181) by t, and defining a new variable $y = I{\cdot}t$, one gets:

$$y = I_0\, e^x \left[1 + (b-1)\,\frac{e^x}{\tau}\right]^{-\frac{b}{b-1}}, \quad b \neq 1, \tag{183}$$

which is now a peak-shaped curve. As in the case of TL and LM-OSL peak-shaped curves, the maximum intensity condition can be found by setting $dy/dt = 0$, which yields:

$$x_m = ln(\tau). \tag{184}$$

From Eq. (184) it is clear that $\tau = e^{x_m}$ regardless the order of kinetics, and therefore one can evaluate the variable τ directly from the peak-shaped curve It versus $ln(t)$ (Eq. (183)).

Eq. (183) can be further transformed following the steps presented in section 8. By applying steps 1–3 in that section, we consider the equation for $x = x_m$ and divide the resulting equations to obtain:

$$\frac{y}{y_m} = e^{x-x_m}\left[\frac{1 + \frac{(b-1)\,e^x}{\tau}}{1 + \frac{(b-1)\,e^{x_m}}{\tau}}\right]^{-\frac{b}{b-1}}. \tag{185}$$

Following step 4 in section 8, we use Eq. (184) for the maximum intensity, and Eq. (185) becomes:

$$y = y_m\, e^{(x-x_m)}\left[\frac{1 + (b-1)\,e^{(x-x_m)}}{b}\right]^{-\frac{b}{b-1}}. \tag{186}$$

Eq. (186) now contains the three variables y_m, x_m and b. Two of them y_m, x_m can be directly evaluated from the transformed experimental decay curve, making thus the curve fitting procedure easy and reliable.

The procedure followed in this subsection can be applied to any stimulated luminescence mode (e.g. CW-OSL and CW-IRSL), provided that its representative curve is a featureless decay curve. The resulting peak-shaped curve has the same mathematical form as Eq. (186) in all cases, with the only difference being the meaning of the decay constant λ.

The TL-like presentation of a decay curve, although very practical and effective, has not found a wide application in research. Some application examples were given by Borchi et al. (1996); Kitis and Otto (1999).

Examples of TL like presentation of experimental data are shown in Fig. 25 for the important dosimetric material (see Fig. 26)Al_2O_3: C.

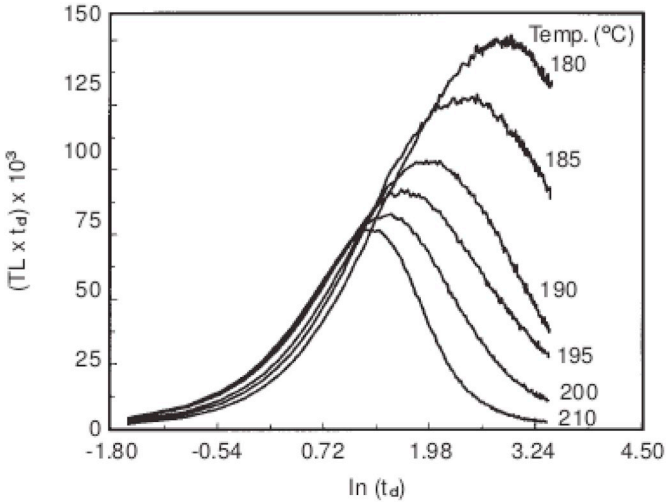

Fig. 25. TL-like presentation of isothermal decay curves of Al_2O_3:C, at various isothermal decay temperatures for time 40 s. After Kitis and Otto (1999).

11.2. Pseudo- LM-OSL presentation

In the case of CW-OSL signals, Bulur (2000) transformed the first order decay curve into a peak-shaped curve, thus obtaining a pseudo-LM-OSL curve. Bulur (2000) introduced a new variable u which is defined as:

$$u = \sqrt{2\,t\,P}\,, \tag{187}$$

or $\left(t = \frac{u^2}{2P}\right)$, where P is the total stimulation time.

For the case of general order kinetics, one substitutes Eq. (187) into Eq. (181), and after multiplying both sides by u/P one obtains:

$$I(t)\,\frac{u}{P} = I(u) = I_0\,\frac{u}{P}\left[1 + (b-1)\,\frac{\lambda\,u^2}{2\,P}\right]^{-\frac{b}{b-1}}. \tag{188}$$

This equation is identical to Eq. (162) for LM-OSL signals, and Bulur (2000) termed as Eq. (188) a pseudo-LM-OSL curve. For an example, the readers could refer to Fig. 26.

By following the transformation steps of section 8, Eq. (188) can be transformed into a form identical to that of Eq. (175), which holds for the general order kinetics LM-OSL.

The same situation holds also for mixed order kinetics. The analytical expressions for pseudo-LM-OSL transformation in the MOK model are exactly similar with those presented in section 8.2.3 (see Kitis et al., 2009)

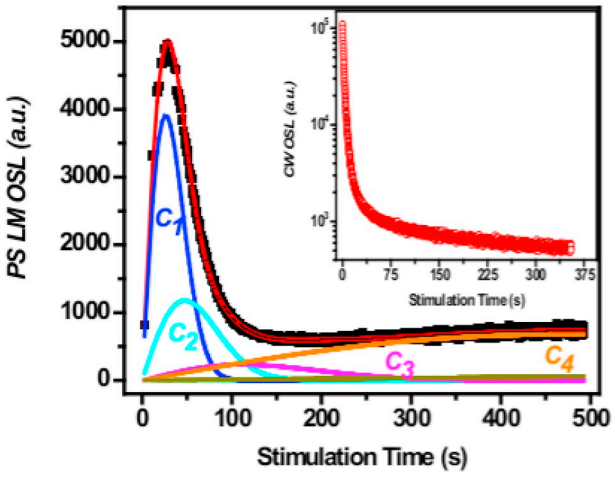

Fig. 26. CGCD of a PS-LM-OSL curve, resulting from the transformation of the respective CW-OSL data shown in the inset. After Kitis et al. (2011).

12. Phenomenological models and the superposition principle: competition effects

12.1. The superposition principle

Experimental luminescence signals are in general complex curves, which can be described as the sum of an appropriate number of individual components. This fundamental idea is based on the assumption that the superposition principle (SP) holds. The SP postulates that every component in the system is independent of the others.

In physics, the SP states that for all linear systems, the net response at a given place and time caused by two or more stimuli, is the sum of the response that would have been caused by each stimulus individually (Wolfson, 2016). Mathematically, for an input x and a response $y = f(x)$, the superposition of the input should yield the superposition of the respective responses, i.e.,

$$f(x_1 + x_2 + \ldots x_n) = f(x_1) + f(x_2) + \ldots + f(x_n). \tag{189}$$

However, the systems of equations studied in this paper are non-linear, and competition effects between the various traps and centers causes them to be inter-correlated, so that the SP principle of Eq. (189) is not fulfilled.

The validity of the extracted information from luminescence signals by using the master equations in this paper, depends on the fulfillment of the SP. In the next subsection we discuss the SP in relation to competition effects.

12.2. The effect of competition on the applicability of the SP- applicability of the quasi-superposition principle (QSP)

The non-fulfillment of the SP can have important consequences on the reliability of the information extracted from the luminescence signals of any SL phenomena. This topic was examined in detail in the simulations by Sadek and Kitis (2018).

A very usual argument one finds in the literature is that CCD analysis is valid only for first order kinetics (Chen and McKeever, 1997; Bøtter-Jensen et al., 2003; Yukihara and McKeever, 2011). In these arguments, first order kinetics is discussed in terms of the Randall - Wilkins first order kinetics equation, which has its origin in the assumption of no-retrapping taking place in the material, and therefore in the absence of any competition between traps and centers. In our opinion, the Randall-Wilkins equation has no relation with the prevalence of the first order kinetics observed in nature. Pagonis and Kitis (2012) showed by extensive simulations, that first order kinetics prevails in nature due to the strong competition effects taking place in any dosimetric material. Typical results of their simulations are shown in Fig. 27. Pagonis and Kitis (2012) showed that as the number of competitors M in an IMTS model is increased, the *shape* of the simulated TL glow curves will approach closer to first order kinetics $b = 1$.

The Randall-Wilkins first order equation is unrealistic, and cannot represent real dosimetric materials during the irradiation stage. The reason is that if all traps in a multi-trap system have negligible retrapping, then no electrons can be trapped in the dosimetric traps during irradiation, and therefore no luminescence signal will be observed during the heating stage. A much more realistic model is provided even by the simplest OTOR model (Halperin and Braner, 1960), from which first order results after making certain simplifying physical assumptions.

Kitis et al. (2017) and Sadek and Kitis (2018) performed extensive simulations, and showed that first order kinetics originates from strong competition effects among active dosimetric traps. These authors found that the competition among traps affects strongly the shapes of TL glow curves in a typical dosimeter. Specifically these authors studied the impact of competition effects on the initial rise method and on the

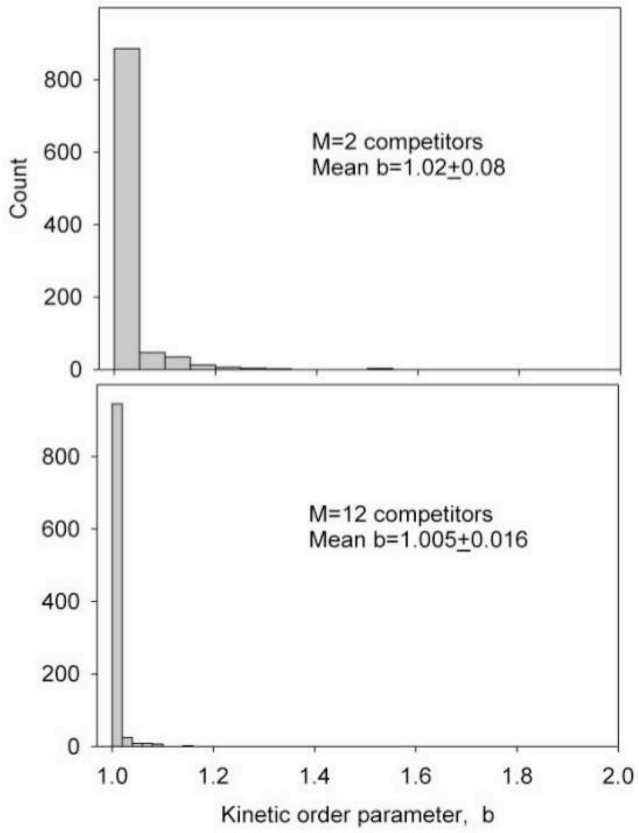

Fig. 27. Simulation of the kinetic order b for $N = 1000$ random variants of the IMTS model and for increasing number M of competitors, as described in the text. Two cases are shown, for $M = 2$ and $M = 12$. After Pagonis and Kitis (2012).

results of CCD analysis. The simulations by Sadek and Kitis (2018) were carried out in a system of five active TL traps in the temperature region used in all practical application (namely between 300 and 700 K).

The simulation results obtained by Sadek and Kitis (2018) were very clear and can be summarized as follows:

In the presence of very strong competition, the following hold:

- The shape of the TL glow curves for the system of five active traps, remains stable as a function of the irradiation dose.
- The active traps follow closely first order kinetics.
- The competition among the active traps is completely eliminated under the conditions of strong competition.
- The curve fitting obtained by CCD is excellent, and
- The output values of the kinetic parameters E, s, n_0 evaluated by the fitting, reproduce with very high accuracy the input values from the model.

Based on these simulation results, Sadek and Kitis (2018) argued that a *quasi-superposition principle* (QSP) holds for real dosimetric materials, because of the strong competition effects present among traps and centers. The important consequence of the QSP being fulfilled, the results of the CCD analysis have to be considered as reliable, and the method can be applied successfully and reliably to experimental TL glow curves.

Sadek and Kitis (2018) simulated also many cases of varying degrees of competition effects, and they observed each time a different degree of fulfillment of the SP. These additional results are summarized as follows. When the competition from TDDT weakens, then the competition effects take place among the active traps, instead of between the traps and the competitors. In such cases of weak competition, the shape of the TL glow curve varies widely. However, even in these cases the curve fitting obtained by the CCD method was excellent, and the CCD analysis in most cases can reproduce the input values of the trapping parameters with high accuracy. These authors also found that the peak area of each component obtained from the CCD analysis, varied strongly from the input values n_0 in the model. This means that in cases of weak competition, the CCD analysis does not reproduce correctly the input values of n_0 of each active trap. The question then arises, what is the impact of these simulation results in dosimetric applications? In our opinion, the answer depends on the experimental conditions of the dosimetric application.

The application of TL in radiation dosimetry is not an absolute dose evaluation method, and the TL dosimeters have to be calibrated relative to known doses. Before a TL measurement, the dosimeters are usually subjected to a regimen of thermal and/or optical preconditioning. A very good example are the pre- and post-irradiation annealing conditioning in LiF dosimeters (Horowitz, 1984), which ensures high stability of the TL glow curves in a wide region of doses. When CCD analysis is applied to the TL glow curves of this material, one is always analyzing the same shape of glow curves. This is true not only for experiments using a linear heating rate, but also for the exponential heating function in a stable temperature hot gas TL reader (Kitis et al., 2012). Therefore, due to the strict preconditioning of the samples and the applicability of the QSP, the CCD analysis becomes a very reliable method of analyzing thermally and optically stimulated signals, as witnessed by its long successful history of practical applications in dosimetry.

12.3. Detecting the existence of SP in experimental curves

A transition is considered *delocalized* when the trapped electrons are stimulated into the conduction band, and subsequently recombine with holes in luminescence centers. By contrast, when the trapped electrons are excited to a higher energy level located below the conduction band, from which they recombine directly with holes in luminescence centers, the transition is considered *localized* (Pagonis et al., 2017).

The applicability of the SP in phenomenological models involving *delocalized* transitions is a debatable issue. However, this issue should not be present for *localized* models, where the donor-acceptor pairs are likely to behave independently of each other. One might expect then, that the SP will be applicable in *localized* models to a greater degree than in *delocalized* models.

In experimental situations, there is practically no available criterion to decide if the constituent components in a luminescence signal are due to delocalized or localized transitions. Therefore, there is also no criterion available to decide whether the SP is fulfilled, or not.

The simulation study by Sadek and Kitis (2018) showed that when the competition from TDDT weakens, the competition effects are transferred to competition between the active traps. As mentioned above, in these cases the TL glow curve *shape* should vary strongly as a function of the irradiation dose. In our opinion, this theoretical prediction is the only criterion available for detecting the fulfillment (or not) of the SP in experimental luminescence signals.

13. Conclusions

The present article provides an extended review on the current status of knowledge concerning the analytical equations/expressions that describe the various stimulated luminescence emissions. For the case of five different well established models, master analytical equations are collected within the same manuscript. As these expressions include the term p, which describes the stimulation mode, the general equations are the same for peak shaped TL and LM-OSL curves as well as decaying OSL, IRSL and ITL curves; this is the reason why these are termed master equations. The majority of these equations use the Lambert-W function, which can be found as a built-in mathematical

function in many commercial mathematical analysis software packages. Therefore, using these master equations for luminescence curve analysis becomes quite easy. The authors strongly encourage the luminescence community to exploit the usefulness of these equations for luminescence signal analysis. Finally, the authors believe that the next step includes incorporating these master equations to either the analysis software packages which are attached to commercial luminescence readers or the recently adopted R-Luminescence software package (Peng et al., 2013, 2016).

Appendix A. Supplementary data

Supplementary data to this article can be found online at https://doi.org/10.1016/j.apradiso.2019.05.041.

References

Adirovitch, E.I., 1956. La formule de Becquerel et la loi elementaire du declin de la luminescence des phosphores crystallins. J. Phys. Radium 17, 705–707.

Balian, H.G., Eddy, N.W., 1977. Figure of Merit(FOM): an improved criterion over the normalized chi-squared test for assessing the goodness-of-fit of gamma ray spectral peaks. Nucl. Instrum. Methods 145, 389–395.

Barry, A.A., Parlang, J.Y., Li, L., Prommer, H., Cunningham, C.J., Stagnitti, F., 2000. Analytical approximations for real values of the Lambert W-function. Math. Comput. Simulat. 53, 95–103.

Borchi, E., Furetta, C., Kitis, G., Leroy, C., Sussman, R.S., Whitehead, A.J., 1996. Assessment of CVD diamond as a thermoluminescence dosemeter material. Radiat. Protect. Dosim. 65, 291–295.

Bøtter-Jensen, L., McKeever, S.W.S., Wintle, A.G., 2003. Optically Stimulated Luminescence Dosimetry. Elsevier Science B.V.

Böhm, M., Scharmann, A., 1981. Theory. In: Oberhofer, M., Scharmann, A. (Eds.), Applied Thermoluminescence Dosimetry, into. Adam Hilger Ltd, pp. 11–38 Bristol.

Bos, A.J.J., Piters, T.M., Gomez Ros, J.M., Delgado, A., 1993. An intercomparison of glow curves analysis computer programs: I. Synthetic glow curves. Radiat. Protect. Dosim. 51, 257–264.

Bos, A.J.J., Piters, T.M., Gomez Ros, J.M., Delgado, A., 1994. An intercomparison of glow curves analysis computer programs: II. Measured glow curves. Radiat. Protect. Dosim. 47, 473–477.

Bos, A.J.J., Wallinga, J., 2009. Optically stimulated luminescence signal under various stimulation modes assuming first-order kinetics. Phys. Rev. B 79, 195118.

Bos, A.J.J., 2017. Thermoluminescence as a research tool to investigate luminescence mechanism. Materials 10, 1357–1379.

Boyd, J.P., 1998. Global approximations to the principal real-values branch of the Lambert W-function. Appl. Math. Lett. 11 (6), 27–31.

Braunlich, P., 1979. Basic principles. In: Braunlich, P. (Ed.), Thermally Stimulated Relaxation in Solids. Springer-Verlag, Berlin, pp. 1–33.

Bull, R.K., 1989. Kinetics of the localized transition model for vthermoluminescence. J. Phys. D Appl. Phys. 22, 1375–1379.

Bulur, E., 1996. An alternative technique for optically stimulated (OSL) experiment. Radiat. Meas. 26, 701–709.

Bulur, E., Goksu, H.Y., 1999. Infrared (IR) stimulated luminescence from feldspars with linearly increasing excitation light intensity. Radiat. Meas. 30, 505–512.

Bulur, E., 2000. A simple transformation for converting CW-OSL to LM-OSL curves. Radiat. Meas. 32, 141–145.

Chen, R., 1969a. On the calculation of activation energies and frequency factors from glow curves. J. Appl. Phys. 40, 570–585.

Chen, R., 1969b. Glow curves with general order kinetics. J. Electrochem. Soc. 116, 1254–1257.

Chen, R., Winer, S.A.A., 1970. Effects of various heating rates on glow curves. J. Appl. Phys. 41, 5227–5232.

Chen, R., 1971. On the remainder of truncated asymptotic series. J. Comput. Phys. 8, 156–161.

Chen, R., 1974. The computation of the exponential integral as related to the analysis of thermal processes. J. Therm. Anal. 6, 585–586.

Chen, R., Kirsh, Y., 1981. Analysis of Thermally Stimulated Relaxation Processes. Pergamon press.

Chen, R., Kristianpoller, N., N Davidson, Z., Visocekas, R., 1981. Mixed first and second order kinetics in thermally stimulated processes. J. Lumin. 23, 293–303.

Chen, R., McKeever, S.W.S., 1997. Theory of Thermoluminescence and Related Phenomena. World Scientific.

Chen, R., Pagonis, V., 2008. A unified presentation of thermoluminescence (TL) phosphorescence and linear-modulated optically stimulated luminescence (LM-OSL). J. Phys. D Appl. Phys. 41, 035102.

Chen, R., Pagonis, V., 2011. Thermally and Optically Stimulated Luminescence. A Simulation Approach Wiley, 2011.

Corless, R.M., Gonnet, G.H., Hare, D.G.E., Jeffrey, D.J., Knuth, D.E., 1996. On the Lambert W function. Adv. Comput. Math. 5, 329–359.

Corless, R.M., Jeffrey, D.J., Knuth, D.E., 1997. A sequence series for the Lambert W function. Proceedings of the International Symposium on Symbolic and Algebraic Computation. ISSAC, pp. 133–140.

Daniels, F. Boyd, C. Saunders, 1953. D. Thermoluminescence as a research tool. Science 117, 343–349.

Dijk van, J.W.E., Julius, H.W., 1993. Glow-curve analysis for constant temperature hot gas TLD readers. Radiat. Protect. Dosim. 47, 479–482.

Dijk van, J.W.E., Busscher, A.I., 2002. The zero signal and glow curves of bare LiF:Mg, Ti detectors in a hot gas TLD system. Radiat. Protect. Dosim. 101, 59–74.

Furetta, C., Weng, P.S., 1998. Operational Thermoluminescence Dosimetry. World Scientific 1998.

Furetta, C., 2003. Handbook of Thermoluminescence. World Scientific 2003.

Garlick, G.F.J., Gibson, A.F., 1948. The electron trap mechanism of luminescence in sulfide and silicate phosphors. Proc. Phys. Soc. Lond. 60, 574–590.

Gomez Ros, J.M., Delgado, A., Bøtter-Jensen, L., Jorgensen, F., 1993. A glow curve analysis method for non-linear heating hot gas readers. Radiat. Protect. Dosim. 47, 483–487.

Gomez-Ros, J.M., Kitis, G., 2002. Computerized glow-curve deconvolution using mixed and general order kinetics. Radiat. Protect. Dosim. 101, 47–52.

Golicnik, M., 2012. On the Lambert W function and its utility in biochemical kinetics. Biochem. Eng. J. 63, 116–123.

Halperin, A., Braner, A.A., 1960. Evaluation of thermal activation energies from glow curves. Phys. Rev. 117, 408–415.

Horowitz, Y.S., 1984. Thermoluminescence and Thermoluminescence Dosimetry, I,vols. II,III CRC press, Boca Raton.

Horowitz, Y.S., Yossian, D., 1995. Computerized glow curve deconvolution: application to thermoluminescence dosimetry. Radiat. Protect. Dosim. 60, 1–114.

Jain, M., Guralnik, B., Andersen, M.T., 2012. Stimulated luminescence emission from localized recombination in randomly distributed defects. J. Phys. Condens. Matter 24, 385402.

Kelly, P.J., Laubitz, M.J., Braunlich, P., 1968. Exact solution of the kinetic equations governing thermally stimulated luminescence and conductivity. Phys. Rev. B 4, 1960–1968.

Kelly, P.J., Braunlich, P., 1970. I. Phenomenological theory of TL. Phys. Rev. B 1, 1587–1595.

Kirsh, Y., Chen, R., 1991. Analysis of blue phosphorescence of X-irradiated albite using a TL-like presentation. Nucl. Tracks Radiat. Meas. 18, 37–40.

Kitis, G., Gomez - Ros, J.M., Tuyn, J.W.N., 1998. Thermoluminescence glow Curve Deconvolution functions for first, second and general order kinetics. J. Phys. D Appl. Phys. 31, 2666 2646.

Kitis, G., Furetta, C., Pagonis, V., 2009. Mixed-order kinetics model for optically stimulated luminescence. Mod. Phys. Lett. B 27, 3191–3207.

Kitis, G., Gomez - Ros, J.M., 1999. Glow Curve Deconvolution functions for mixed order kinetics and a continuous trap distribution. Nucl. Instrum. Methods A 440, 224–231.

Kitis, G., Otto, T., 1999. Isothermal decay readout: application to LiF:Mg,Ti and α-Al_2O_3:C. Radiat. Prot. Dosim. 86, 181–190.

Kitis, G., Chen, R., Pagonis, V., Carinou, E., Kamenopoulou, V., 2006a. Thermoluminescence under an exponential heating function: I. Theory. J. Phys. D: Appl. Phys. 39, 1500–1507.

Kitis, G., Chen, R., Pagonis, V., Carinou, E., Ascounis, P., Kamenopoulou, V., 2006b. Thermoluminescence under an exponential heating function: II. Glow-curve deconvolution of experimental glow-curves. J. Phys. D Appl. Phys. 39, 1508–1514.

Kitis, G., Pagonis, V., 2007. Peak shape methods for general order thermoluminescence glow-peaks: a reappraisal. Nucl. Instrum. Methods Phys. Res. B 262, 313–323.

Kitis, G., Chen, R., Pagonis, V., 2008. Thermoluminescence glow-peak shape methods based on mixed order kinetics. Phys. Status Sol.(a) 205, 1181–1189.

Kitis, G., Pagonis, V., 2008. Computerized curve deconvolution analysis for LM-OSL Radiat. Meas 43, 737–741.

Kitis, G., Polymeris, G.S., Kiyak, N.G., Pagonis, V., 2011. Preliminary results towards the equivalence of transformed continuous - wave optically stimulated luminescence (CW-OSL) and linearly-modulated (LM-OSL) signals in quartz. Geochronometria 38, 209–216.

Kitis, G., Carinou, E., Askounis, P., 2012. Glow-curve de-convolution analysis of TL glow-curves from constant temperature hot gas TLD readers. Radiat. Meas. 47, 258–265.

Kitis, G., Vlachos, N.D., 2013. General semi-analytical expressions for TL,OSL and other luminescence stimulation modes derived from OTOR model using the Lambert W - function. Radiat. Meas. 482, 47–54.

Kitis, G., Pagonis, V., 2013. Analytical solution for stimulated luminescence emission from tunneling recombination in randomly distributions of defects. J. Lumin. 137, 109–115.

Kitis, G., Pagonis, V., 2014. Properties of thermoluminescence glow curves from tunneling recombination in random distributions of defects. J. Lumin. 153, 118–124.

Kitis, G., Polymeris, G.S., Sahiner, E., Meric, N., Pagonis, V., 2016a. Influence of the infrared stimulation of the optically stimulated luminescence in four K-feldspar samples. J. Lumin. 176, 32–39.

Kitis, G., Polymeris, G.S., Sfampa, I.K., Prokic, M., Meric, N., Pagonis, V., 2016b. Prompt isothermal decay of thermoluminescence in MgB_4O_7:Dy,Na and :LiB_4O_7:Cu,In dosimeters. Radiat. Meas. 84, 15–25.

Kitis, G., Pagonis, V., Tzamarias, E.S., 2017. The influence of competition effects on the initial rise method during thermal stimulation of luminescence: a simulation study. Radiat. Meas. 100, 27–36.

Kitis, G., Pagonis, V., 2018. Localized transition models in luminescence: a reappraisal. Nucl. Instrum. Methods Phys. Res. B 432, 13–19.

Klein, M.J., 1955. Principles of detailed balance. Phys. Rev. 97 (6), 1446–1447.

Lawless, J.L., Lo, D., 2001. Thermoluminescence for nonlinear heating profiles with application to laser heated emissions. J. Appl. Phys. 89, 6145–6152.

Lawless, J.L., Chen, R., Lo, D., Pagonis, V., 2005. A model for non-monotonic dose dependence of thermoluminescence (TL). J. Phys. Condens. Matter 17, 737–753.

Lewandowski, A.C., McKeever, S.W.S., 1991. Generalized description of thermally

stimulated processes without quasiequilibrium approximation. Phys. Rev. B 43, 8163–8178.
Lloyd, J.P., Pake, G.E., 1954. Spin relaxation in free radical solutions exhibiting hyperrfine structure. Phys. Rev. 94 (3), 579–591.
Lovedy Singh, L., Gartia, R.K., 2013. Theoretical derivation of a simplified form of the OTOR/GOT differential equation. Radiat. Meas. 59, 160–164.
Mandowski, A.J., 2005. Semi-localized transitions models for thermoluminescnce. J. Phys. D Appl. Phys. 38, 17–21.
Martini, M., Meinardi, F., 1997. Thermally stimulated luminescence: new perspectives in the study of defects in solids, 1997. Riv. Nuovo Cimento 20, 1–71.
May, C.E., Partridge, J.A., 1964. TL kinetics of alpha irradiated alkali halides. J. Chem. Phys. 40, 1401–1409.
McKeever, S.W.S., Chen, R., 1997. Luminescence models invited review paper, special issue on luminescence dating. Radiat. Meas. 27, 625–661.
Oniya, E.O., Polymeris, G.S., Tsirliganis, N.C., Kitis, G., 2012. Radiation dose response correlation between thermoluminescence and optically stimulated luminescence in quartz. J. Lumin. 132, 1720–1728.
Opanowicz, A., 1992. Effect of initial trap occupancy on thermoluminescence characteristics of insulating crystals. Phys. Stat. Sol. A 130, 207–217.
Osada, K., 1960. Thermoluminescence of Zinc sulfide phosphors. J. Phys. Soc. Jpn. 15, 145–149.
Pagonis, V., Kitis, G., Furetta, C., 2006. Numerical and Practical Exercises in Thermoluminescence. Springer, New York, NY, USA 2006; ISBN 0-387-26063-3.
Pagonis, V., 2005. Evaluation of activation energies in the semi-localized transition model of thermoluminescence. J. Phys. D Appl. Phys. 38, 2179.
Pagonis, V., Kitis, G., 2012. Prevalence of first order kinetics in thermoluminescence materials: an explanation based on multiple competition processes. Phys. Status Solidi B 249, 1590–1601.
Pagonis, V., Phan, Huy, Ruth, D., Kitis, G., 2013. Further investigations of tunneling recombination processes in random distribution of defects. Radiat. Meas. 58, 66–74.
Pagonis, V., Kitis, G., 2015. Mathematical aspects of ground state tunneling models in luminescence materials. J. Lumin. 168, 137–144.
Pagonis, V., Chen, R., Kulp, C., Kitis, G., 2017. An overview of recent developments in luminescence models with focus on localized transitions. Radiat. Meas. 106, 3–12.
Peng, J., Dong, Z.B., Han, F.Q., Long, H., Liu, X.J., 2013. R-package numOSL: numeric routines for optically stimulated luminescence dating. Ancient TL 31 (2), 41–48.
Peng, J., Dong, Z., Han, F., 2016. tgcd: an R package for analyzing thermoluminescence glow curves. Software X 5, 112–120.
Piters, T.M., Bos, A.J.J., 1993. Success and failure of the Randall-Wilkins model for thermoluminescence in LiF(TLD). Radiat. Protect. Dosim. 47, 41–47.
Podgorsak, E.B., Moran, P.R., Cameron, J.R., 1971. Interpretation of resolved glow—curves shapes in LiF(TLD-100) from 100K to 500K. In: Proc. 3rd Conf, on Luminescence Dosimetry, Riso Report 249 (Denmark:IAES and Danish AEC) p.1.
Polymeris, G.S., Pagonis, V., Kitis, G., 2017. Thermoluminescence glow curves in preheated feldspar samples: an interpretation based on random defect distribution. Radiat. Meas. 97, 20–27.
Randall, J.T., Wilkins, M.H.F., 1945a. Phosphorescence and electron traps I. The study of trap distributions. Proc. Roy. Soc. Lond. 184, 366–389.
Randall, J.T., Wilkins, M.H.F., 1945b. Phosphorescence and electron traps II. The interpretation of long-period phosphorescence. Proc. Roy. Soc. Lond. 184, 390–407.
R Core Team, 2014. R: A Language and Environment for Statistical Computing. R Foundation for Statistical Computing URL. http://www.Rproject.org/.
Rasheedy, M.S., 1993. On the general-order kinetics of the thermoluminescence glow peak. J. Phys. Condens. Matter 5, 633–636.
Sadek, A.M., Eissa, H.M., Basha, A.M., Kitis, G., 2014a. Resolving the limitation of peak fitting and peak shape methods in determinations of the activation energy of thermoluminescence glow peaks. J. Lumin. 146, 418–423.
Sadek, A.M., Eissa, H.M., Basha, A.M., Kitis, G., 2014b. Development of peak fitting and peak shape methods to analyze the thermoluminescence glow-curves generated with exponential heating function. Nucl. Instrum. Methods Phys. Res. B 330, 103–107.
Sadek, A.M., Eissa, H.M., Basha, A.M., Kitis, G., 2015a. The deconvolution of thermoluminescence glow-curves using general expressions derived from the one trap-one recombination (OTOR) level model. Appl. Radiat. Isot. 95, 214–221 2015.
Sadek, A.M., Eissa, H.M., Basha, A.M., Kitis, G., 2015b. Properties of the thermoluminescence glow peaks simulated by the interactive multi trap system (IMTS) model. Phys. Status Solidi B 252, 721–729.
Sadek, A.M., Kitis, G., 2017. A critical look at the kinetic parameter values used in simulating the thermoluminescence glow-curve. J. Lumin. 183, 533–541.
Sadek, A.M., Kitis, G., 2018. Impact of non-fulfillment of the super position principle on the analysis of thermoluminescence glow-curve. Radiat. Meas. 116, 14–23.
Sahiner, E., Meriç, N., Polymeris, G.S., 2014. Assessing the impact of IR stimulation at increasing temperatures to the OSL signal of contaminated quartz. Radiat. Meas. 68, 14–22.
Sahiner, E., 2017. Deconvolution analysis of thermoluminescent glow curves in various commercial dosimeters using two different approaches in the framework of the one-trap, one-recombination model. Turk. J. Phys. 41, 477–490. https://doi.org/10.3906/z-1704-25.
Sfampa, I.K., Polymeris, G.S., Tsirliganis, N.C., Pagonis, V., Kitis, G., 2014. Prompt isothermal decay of thermoluminescence in an apatite exhibiting strong anomalous fading. Nucl. Inst. Meth. in Phys. Reas. B 320, 57–63.
Sunta, C.M., Feria Ayta, W.E., Piters, T.M., Watanabe, S., 1999. Limitation of peak fitting and peak shape methods for determination of activation energy of thermoluminescence glow peaks Radiat. Meas 30, 197–201.
Sunta, C.M., Ayta, W.E.F., Chubaci, J.F.D., Watanabe, S., 2001. A critical at the kinetic models of thermoluminescence: I. First-order kinetics. J. Phys. D 34, 2690–2698.
Sunta, C.M., Ayta, W.E.F., Chubaci, J.F.D., Watanabe, S., 2002a. General order and mixed order fits of thermoluminescence glow curves - a comparison. Radiat. Meas. 35, 47–57.
Sunta, C.M., Ayta, W.E.F., Chubaci, J.F.D., Watanabe, S., 2002b. Test for quasi-equilibrium in thermally stimulated luminescence and conductivity. Radiat. Meas. 35, 595–602.
Sunta, C.M., Ayta, W.E.F., Chubaci, J.F.D., Watanabe, S., 2005. A critical look at the kinetic models of thermoluminescence -II. Non-first order kinetics. J. Phys. D 38, 95–102.
Templer, R., 1986. The localized transition model of anomalous fading. Radiat. Protect. Dosim. 17, 493 397.
Thomsen, J., 1953. Logical relations among the principles of statistical mechanics and thermodynamics. Phys. Rev. 91 (5), 1263–1266.
Valluri, S.R., Jeffrey, D.J., Corless, R.M., 2000. Some applications of the Lambert W function in. Physics Canadian Journal of Physics 78, 823–831.
Visocekas, R., 1985. Tunneling radiative recombination in labradorite: its association with anomalous fading of thermoluminescence. Nucl. Tracks 10, 521–529.
Visocekas, R., 1988. Comparison between tunneling afterglow following alpha and beta irradiations. Nucl. Tracks Radiat. Meas. 14, 163–168.
Visocekas, R., Spooner, N.A., Zink, A., Blank, P., 1994. Tunnel afterglow, fading and infrared emission in thermoluminescence of feldspars. Radiat. Meas. 23, 377–385.
Wintle, A.G., 1977. Detailed study of a thermoluminescent mineral exhibiting anomalous fading. J. Lumin. 15, 385–393.
Wolfson, R., 2016. Facts101:Essential University Physics. Cram101 Textbook Reviews.
Yossian, D., Horowitz, Y.S., 1997. Mixed order and general order kinetics applied to synthetic glow peaks and peak 5 in LiF:Mg. T. Radiat. Meas. 25, 465–471.
Yukihara, E., McKeever, S.W.S., 2011. Optically Stimulated Luminescence: Fundamentals and Applications, 2011. John Wiley Sons Ltd.